Legault Geoffrey (Orcid ID: 0000-0003-2136-587X)
Shah Alisha A. (Orcid ID: 0000-0002-8454-7905)
Larkin Beau G. (Orcid ID: 0000-0001-8387-7315)

Climate-driven thermal opportunities and risks for leaf miners in aspen canopies

H. Arthur Woods[1], Geoffrey Legault[2], Joel G. Kingsolver[2], Sylvain Pincebourde[3], Alisha A. Shah[1,5], Beau G. Larkin[4]

[1]Division of Biological Sciences, University of Montana, Missoula, MT 59812 USA, [2]Department of Biology, University of North Carolina, Chapel Hill, NC 27599, USA, [3]Institut de Recherche sur la Biologie de l'Insecte, UMR 7261, CNRS - Université de Tours, 37200 Tours, France, [4]MPG Operations, LLC, 1001 South Higgins Ave, Suite 3A, Missoula, MT 59801 USA, [5]W.K. Kellogg Biological Station, Department of Integrative Biology, Michigan State University, Hickory Corners, MI, USA

Corresponding author: H. Arthur Woods. E-mail: art.woods@mso.umt.edu

Open Research Statement: Data (Woods, et al. 2022a) are available from Dryad at https://doi.org/10.5061/dryad.d2547d84j. Scripts (Woods, et al. 2022b) underlying the figures in this manuscript are archived in Zenodo at https://doi.org/10.5281/zenodo.6613812.

Abstract

In tree canopies, incoming solar radiation interacts with leaves and branches to generate temperature differences within and among leaves, presenting thermal opportunities and risks for leaf-dwelling ectotherms. Although leaf biophysics and insect thermal ecology are well understood, few studies have examined them together in single systems. We examined temperature variability in aspen canopies, *Populus tremuloides*, and its consequences for a common herbivore, the leaf-mining caterpillar *Phyllocnistis populiella*. We shaded leaves in the field and measured effects on leaf temperature and larval growth and survival. We also estimated larval thermal performance curves for feeding and growth and measured upper lethal temperatures. Sunlit leaves directly facing the incoming rays reached the highest temperatures, typically 3 – 8 °C above ambient air temperature. Irradiance driven increases in temperatures, however, were transient enough that they did not alter observed growth rates of leaf miners. Incubator and ramping experiments suggested that larval performance peaks between 25 and 32 °C and declines to zero between 35 and 40 °C, depending on duration of temperature exposure. Upper lethal temperatures during one-hour heat shocks were 42 – 43 °C. When larvae were active in early spring, temperatures generally were low enough to depress rates of feeding and growth below their maxima, and only rarely did estimated mine temperatures rise beyond optimal temperatures. Observed leaf or mine temperatures never approached larval upper lethal temperatures. At this site during our experiments, larvae thus appeared to have a significant thermal safety margin; the more pressing problem was inadequate heat. Detailed information on mine temperatures and larval performance curves, however, allowed us to leverage long-term data sets on air temperature to estimate potential future shifts in performance and longer-term risks to larvae from lethally high temperatures. This analysis suggests that, in the past 20 years, larval performance has often been limited by cold and that the risk of heat stress has been low. Future warming will raise mean rates of feeding and growth but also the risk of exposure to injuriously or lethally high temperatures.

Key words: aspen, climate change, critical thermal limits, growth, leaf miner, microclimate, plant-insect interactions, temperature, thermal performance curve

Introduction

Small, terrestrial ectotherms live in climatic conditions occurring at small spatial scales (microclimates) immediately around the organism (Pincebourde and Woods 2020), which arise as broader-scale climates interact with objects in the local ecosystem, including plants, rocks, soils, water, and other animals (Woods, Dillon, and Pincebourde 2015). Because the arrangement, size, and properties of those objects can be complex, microclimatic variation can be high, even over relatively small spatial extents. For example, variation in surface temperatures within a few square meters may exceed variation in air temperatures at 2 m height occurring across hundreds or thousands of kilometers (Helmuth et al. 2006; Scherrer and Körner 2010). Similarly, steep gradients in air temperature may exist over just a few millimeters away from the surfaces of sunlit objects (Kaspari et al. 2015; Pincebourde, Dillon, and Woods 2021; Sommer and Wehner 2012). Quantifying these microclimatic mosaics is key to anticipating ecological responses to environmental changes, especially given that their range can surpass the amplitude of change at regional or global scales.

Among herbivorous insects, especially small ones immersed deeply in boundary layers, body temperatures are strongly influenced by leaf temperatures (Pincebourde and Woods 2012; Pincebourde, Dillon, and Woods 2021; Woods 2013). In turn, leaf temperatures are influenced by a wide variety of climatic factors, plant structural and physiological traits (Campbell and Norman 1998; Dong et al. 2017; Gates 1968; Nobel 1999; Perez and Feeley 2020) and insect activities (Pincebourde and Casas 2019). Leaves of many plants exhibit a kind of 'limited homeothermy' or 'biophysical homeostasis' (Dong et al. 2017; Linacre 1964, 1967; Michaletz et al. 2015, 2016; Potter, Davidowitz, and Woods 2009), in which leaf temperatures (of wellwatered plants) are higher than air temperatures when the air is cool but cooler than air temperatures when the air is warm. Limited homeothermy may provide at least some protection from unsuitable or dangerous temperatures at both cold and hot ends of the temperature distribution (see Potter, Davidowitz, and Woods 2009). In addition, plants often generate strong mosaics of temperature within and among leaves (Jones 1999; Leuzinger and Körner 2007; Pincebourde and Suppo 2016; Saudreau et al. 2017; Woods, Saudreau, and Pincebourde 2018; Miller et al. 2021).

Solar radiation is especially important, as it can dominate local heat budgets of sunlit objects compared to other heat-transporting processes (Gates 1980; Vogel 2009) and can drive enormous variation in temperature —on the order of 10 to 20 °C – in microhabitats relevant to small organisms. This is true for habitats generally (Oke 2002; Sears, Raskin, and Angilletta 2011; Stoutjesdijk 1977) and for variation within and among plants (Kaspari et al. 2015; Linacre 1967, 1964; Pincebourde and Suppo 2016; Woods, Saudreau, and Pincebourde 2018; Miller et al. 2021). Local microclimates may be diverse enough that insects can shift their body temperatures significantly by moving just a few centimeters (Faye et al. 2017; Pincebourde et al. 2016; Willmer 1982; Woods 2013; Woods, Dillon, and Pincebourde 2015; Pincebourde, Dillon, and Woods 2021; Caillon et al. 2014). Another potentially important phenomenon is transient episodes of direct solar radiation in otherwise shaded conditions (sunflecks). Sunflecks can result in many-fold elevations in the intensity of solar radiation arriving at surfaces. The implications for leaf functions are relatively well known: sunflecks may alter the carbon balance of understory plants, and can drive rapid, transient rises in leaf temperature to 10 – 20 °C above ambient air temperature (Schymanski, Or, and Zwieniecki 2013). The implications of sunflecks for insects are less well known, although some species are known to utilize them to raise their body temperatures in otherwise cool habitats (Schultz 1998) or to avoid them in warm habitats (Kaspari et al. 2015; Meisel 2006). The effects of sunflecks on immobile, leaf-dwelling insect herbivores are largely unknown, and we hypothesize that they may constitute a valuable thermal resource in cool environments while raising the risk of overheating in warm environments.

Insects themselves also can drive significant variation in local temperatures both by building structures and by influencing leaf energy budgets. For example, insect feeding damage can alter rates of leaf transpiration (Aldea et al. 2005; Cockfield and Potter 1986; Welter 2019; Zangerl et al. 2002), which can raise or lower temperatures (Pincebourde and Casas 2019). Other species alter local temperatures by building structures (Lill and Marquis 2007), including leaf mines, galls, rolls, and structures made from silked or tied leaves (Henson 1958; Pincebourde and Casas 2006). These physiological and physical manipulations are forms of niche construction (Odling-Smee, Laland, and Feldman 2003; Pincebourde and Casas 2019; Woods et al. 2021). Such species typically do not thermoregulate by moving across the microclimate mosaic but rather by modifying plant tissues to limit overheating in warm conditions or to obtain more heat in cold conditions.

For insect herbivores, the significance of microclimatic variation depends on the distribution of realized insect body temperatures in relation to the thermal performance curve (Figure 1). Compared to shaded surfaces in cool locations or seasons (e.g., early spring), sunlit surfaces can provide suitable or even optimal thermal conditions (T_{OPT}) without imposing a significant risk of reaching critical thermal maxima (CT_{MAX}). By contrast, in hotter locations and times of year, sunlit surfaces may impose significant thermal risk while shaded surfaces remain suitable if not optimal. These relative risks are also modified by whether the insect is mobile. Mobile insects can avoid uncomfortably hot locations, and, indeed, such behaviors may mitigate selection on high-temperature tolerance (Huey, Hertz, and Sinervo 2003; Bogert 1949; Muñoz and Bodensteiner 2019). By contrast, relatively immobile insects – leaf miners, gall makers, stem borers, stages that cannot move including eggs and pupae – may not be able to escape hot conditions and may therefore experience more frequent selection on high-temperature tolerance.

Although biologists increasingly recognize that microclimatic diversity is important (Denny et al. 2011; Kaspari et al. 2015; Pincebourde and Casas 2019; Potter, Woods, and Pincebourde 2013; Perez and Feeley 2020), little is known about actual patterns of microclimatic variation experienced by small ectotherms in the wild, or its consequences for organisms and populations (Kingsolver 1979). We therefore examined a tractable terrestrial system – aspens (*Populus tremuloides*) and one of its common herbivores, the aspen leaf miner (Lepidoptera: *Phyllocnistis populiella*). Larval leaf miners, which spend their entire pre-adult phase on a single aspen leaf, have little or no opportunity for behavioral thermoregulation (though some leaf-mining insects can thermoregulate over very small scales; see (Pincebourde and Casas 2006)). Rather, they depend on choices made by their mothers (Stahlschmidt and Adamo 2013), evolve mechanisms for tolerating more extreme temperatures, or engineer their local microclimates to avoid risk and enhance exposure to optimal conditions (Pincebourde and Casas 2019; Ma, Ma, and Pincebourde 2021; Woods et al. 2021). Our goals are to understand (i) temporal and spatial (microscale) patterns of thermal variation within and among leaves and (ii) the effects of those patterns on the thermal performance of leaf-mining caterpillars, focusing particularly on effects on growth and risk of high-temperature injury arising from sunflecks. In addition, we evaluate how climate warming may affect future performance and thermal risks in tree canopies characterized by complex, highly transient radiative environments (Ma, Ma, and Pincebourde 2021).

Materials and Methods

Study site and species.

The study site was located on a privately owned, 80-hectare study site on the east side of the Swan Valley in Western Montana (47°31'20"N, 113°40'6"W, elevation 1230 m). Historically, vegetation at the site was consistent with the Rocky Mountain dry-mesic montane mixed conifer forest (Vance and Luna 2017), and the primary disturbance was fire. Burns created openings in the forest and allowed quaking aspen (*Populus tremuloides*), a species that grows poorly under the shade of conifers, to persist for centuries. After the current owner purchased the property in 2004, aspen stands were dominated by a few mature stems. Fences were built around existing aspen stands to protect them from herbivory by ungulates, which encouraged the growth of new ramets. In suitable locations, new aspen stands were planted and fenced. After more than 10 years inside these fences, aspen ramets in both existing and planted aspen stands have flourished, creating ideal conditions to study associations between aspens and insects like aspen leaf miners.

Aspens occur broadly across boreal North America and south along the Rocky Mountains and the Sierra Nevada. The herbivore *Phyllocnistis populiella* (Lepidoptera: Gracillariidae) also appears to be broadly distributed (Condrashoff 1964) and can occur at high densities in some sites (Wagner et al. 2008). Adult females of *P. populiella* emerge from leaf litter in spring, find males and mate, and then oviposit on young aspen leaves. The eggs subsequently sink into the leaf tissue and hatch soon after leaves flush in early to mid-May. The caterpillars consume the epidermal cell layer (lying between cuticle and mesophyll) as they grow through four instars (Condrashoff 1964; Wagner et al. 2008), and within several weeks (depending on temperature) they form a pupal case by folding a small edge of the leaf over themselves, which they secure with silk. The pupal stage lasts for approximately one month, after which adults emerge, typically in July. The adults persist through the summer, fall, and winter. Mortality of larvae and pupae from predation and parasitism can be very high (> 50%) in some populations in some years (Condrashoff 1964); at our site, we have observed parasitism rates, by eulophid wasps, of ~ 35% over three years (unpubl. observations).

Because *P. populiella* are confined to single leaves as eggs, larvae, and pupae, they likely cannot engage in significant behavioral thermoregulation. In addition, they occur at moderate densities at our field site in Montana (occurring on 0 – 25% of leaves in aspen saplings), and the damage they cause (each one makes its own silvery mine, Figure 2A) is easy to spot from a distance. At our site, a large majority of mines were on the stomatous abaxial side (underside). This positioning contrasts with populations observed in Alaska, in which most mine damage was on the astomatous adaxial side (Wagner, Wheeler, and Burr 2020).

Climate data collection.

In 2017, we set up a weather station (Campbell Scientific) on the MPG-North property that has been collecting data every minute almost continuously on air temperature, relative humidity, wind direction, and wind speed (from a WS600-UMB weather sensor) at 3.5 m height and precipitation and solar radiation (rotating shadowband radiometer, RSR2) at 2 m height. The station is located at 47°31’24.12”N, 113°40’20.75”W at an elevation of 1213 m, ~ 500 m northwest of our main aspen study site.

Temperature and growth measurements.

Leaf temperatures were measured using thermocouples fixed to leaf surfaces, which provide high frequency temporal time series but poor spatial coverage; and using an infrared imaging camera, which provides high spatial resolution but poor temporal coverage. Leaf temperatures were measured by fixing fine type-T thermocouples (0.13 mm wires) to leaves using a small strip of clear tape placed across the unsoldered base of the thermocouple, near the leaf petiole, with the wire tip bent so that the junction rested against the leaf surface. Thermocouples were connected to Hobo 4-channel data loggers (UX120-014M) sampling every 5 min. Infrared images were obtained with a FLIR T540 camera (464 x 348 pixel, 7.5 – 14 μm sensitivity, 17 mm lens) in either normal or macro mode. Leaf emissivity was assumed to be 0.95, and tests in which leaves were measured simultaneously with thermocouples showed that this value gave a close match, under a variety of conditions, between thermocouple temperature and the temperature estimated by the camera. Leaves or mines were imaged with the infrared camera always from the same distance (~30 cm), to avoid potential systematic shifts in estimated temperature arising from changes in the distance between object and camera (Faye, Dangles, and Pincebourde 2016). Files were exported into the FLIR Tools+ software package (v 6.4.18039.1003) and analyzed using spot and line tools.

Because it is not possible to remove larvae from mines and then to reintroduce them, we could not measure growth rates from direct measurements of change in larval mass. We instead estimated larval mass from mine area by constructing a mass-area calibration curve. We collected 54 mined leaves in 2017 and 106 in 2018. Each was photographed (Nikon D7100 with 105 mm macro lens) in a standard orientation, with a ruler in the field of view, then its larva was extracted and weighed (± 1 μg) on a Sartorius MC-5 microbalance. The area of each mine was estimated in ImageJ (v. 1.52A) by first setting the scale of the image from the ruler then by tracing around the mine with the polygon selection tool. Larval mass was regressed against mine area, and the relationship was modeled using least-squares regression.

Effects of sun versus shade on leaf temperatures and caterpillar growth.

A primary goal was to estimate how solar radiation drives spatial and temporal patterns of temperature variation across aspen canopies, and to assess the consequences of that variation for caterpillar growth. We assessed the importance of solar radiation by comparing leaf temperatures and caterpillar growth rates in pairs of mines, one exposed to natural light and the other experimentally shaded.

The experiment was run twice, both times for three days. The first experiment was started on May 21, 2018, with 16 pairs of mines. Pairs were located < 1.5 m height from the ground on the south sides of aspen saplings at MPG North (1 pair per tree, with one mine of the pair experimentally shaded and the other not). Leaves had steep leaf angles (hanging 45 - 90°) vertically from their petioles with faces oriented in a wide distribution of directions. Note that even experimentally unshaded leaves were shaded a significant fraction of the time by other parts of the canopy. Experimental shades consisted of a rectangular piece of foil-covered plastic mounted with a post and bracket (Figure 2D) so that direct sunlight was blocked between 9 am and 4 pm. The other mine of the pair was exposed to natural lighting. Visual images (Olympus Tough TG-5) were taken of each mine on the evening of the first day, then at ~12 h intervals through the morning of May 24. Ten of 16 pairs were fitted with thermocouples as described above. The experiment was run a second time, with new pairs of larvae, starting on May 25, 2018.

During the first experiment, light levels (lux) were measured with pendant light loggers (Onset MX2202) hung vertically (like many leaves) facing south. The spectral response of the loggers closely matches the sensitivity of the human eye (400 – 700 nm, peaking near 550 nm). In addition, logger response varies as a function of angle of illumination, with response falling off approximately as a cosine curve (highest sensitivity with incoming light orthogonal to the sensor surface). Four pairs of loggers were mounted near four haphazardly chosen pairs of experimental leaves, with one logger mounted above the shade (to measure unmanipulated light levels) and the other hanging at leaf height below the shade. Larval growth rates were estimated from images of mine area as described above.

Leaf temperature as a function of angle to the sun.

To infer the thermal diversity generated by leaf geometry variation across canopies, we experimentally altered leaf geometry and measured surface temperature using the thermal imaging camera. In early June 2019, individual leaves (still attached to their tree) were fixed, using small pieces of clear tape, to the central cutout of a small rectangle of plastic. This arrangement permitted airflow around the leaf but prevented leaf fluttering, which likely decreases convective heat transfer between the leaf and air (Roden and Pearcy 1993); our measurements thus provide an upper estimate for potential leaf temperatures under the conditions prevailing on measurement days. The plastic rectangle was mounted to a camera tripod fitted with a protractor, and the leaf was positioned initially with its face orthogonal to the sun (designated as 0°). After waiting several minutes for leaf temperature to stabilize, we imaged it in IR from a distance of ~30 cm. This process was repeated for angles of 30, 60, and 85° to the sun. Leaf temperatures were extracted as the mean temperature from a linear transect across the middle of the leaf, and excess leaf temperatures (T_{excess}) were calculated as T_{leaf} – local T_{air} at the time of measurement.

Leaf temperature of mined versus unmined tissue.

Temperatures of leaf mines may differ systematically from temperatures of unmined tissues and leaves, either because mines act as greenhouses (Pincebourde and Casas 2006) or because larva-leaf interactions alter stomatal opening and therefore local rates of cooling by transpiration (Pincebourde and Casas 2006, 2019). Wagner et al. (2020) examined these potential effects for Alaskan populations and found complex effects of mines on aspen leaf transpiration. When mines were abaxial (the stomatous side), they tended to reduce total water loss by disrupting stomatal function, leading them to close; when mines were adaxial (astomatous), they had no effect on stomatal conductance but increased rates of transpiration through adaxial cuticle. Given that most of the mines in our population are abaxial, we expected mined tissues to show lower rates of transpiration and therefore warming.

We examined these possibilities by imaging 110 aspen leaves in IR on June 4, 2019 (between 13:30 and 15:00), of which 68 were mined. For a subset of these mined leaves (N = 42), we also imaged a nearby unmined leaf with a similar orientation from the same branch within 60 s. For all leaves, we noted, prior to imaging, whether they were in full sun, partial shade, or full shade. We analyzed extracted leaf temperatures in two ways. First, we compared temperatures of mined versus unmined tissues within the same leaves. Second, to examine whether mining affects the temperature of nearby unmined tissues on the same leaf, we compared temperatures of unmined tissues from mined and unmined leaves.

Upper lethal temperatures.

Customized battery-powered heating devices (built by the SensorSpace group at the Flathead Lake Biological Station, Univ. of Montana) were used to heat shock larvae in the field without removing them from their leaves (Figure 2B, C). Each device had an Arduino computer controlling power to a piece of heater tape positioned inside a small, plastic box that was clamped over a single leaf still attached to the tree. Temperature feedback was provided by a thermistor mounted inside the box, and a small computer fan circulated air to minimize internal temperature gradients. The duration and severity of the heat shock was programmable, and the computer logged the realized box temperature (1 Hz). Mine-containing leaves were positioned, using a small piece of tape, so that larvae were directly above the box's thermistor, and additional measurements using fine type T thermocouples confirmed that set and measured temperatures usually were within 0.5 °C of one another.

The devices were used to heat-shock 52 larvae in the field. Shocks were conducted during the daytime, between 9 AM and 5 PM, for one hour at haphazardly chosen temperatures between 38 and 48.4 °C. Heaters generally reached their set points within 5 minutes, and held temperatures to within 0.5 °C of the set point (see Appendix S1: Figure S1). At the end of the hour-long heat shock, the box was removed from the leaf. We then marked the position of the front of the larval mine with a small dot of black Sharpie and photographed the mine (Olympus Tough TG-5). Mines were photographed on the two following days, and images were analyzed to determine whether larvae constructed additional mine area beyond the marked front. Larvae were assumed to be killed by heat shock when the mined area remained unchanged after two days. Often larvae also showed other changes associated with death, including discoloration and shriveling.

Thermal performance curves for growth from short-term incubator experiments.

Growth rates of larvae were measured over single 8-hour periods at different constant temperatures. Mined leaves were collected at MPG North, and their petioles were placed into water ($N = 152$ total, collected over four days to avoided generating confounding changes in leaf characteristics). Leaves were returned the same day to the University of Montana and put overnight into incubators set to a nighttime temperature of 10 °C. The lights came on the following morning at 6 AM, and the daytime temperature went to one of nine temperatures (5, 10, 15, 20, 25, 30, 33, 35, 37 °C, with total *N* per treatment of 11, 21, 18, 27, 18, 27, 9, 14, and 9, respectively). Starting at 8 AM, leaves were removed briefly from their incubator, laid flat on a laboratory bench under a tripod-mounted digital camera (Nikon D7100), and photographed, then were rapidly placed back into their experimental incubator. The imaging process was repeated for each leaf 8 hours later. Larval mass at the beginning and end of the 8-hour growth period was estimated from the imaged mines as described above. Mass-specific growth rates were calculated as final minus initial mass, divided by the initial mass and the total time between measurements.

Thermal performance curves for feeding in acutely imposed temperatures.

Feeding rates of larval miners were also measured for a range of temperatures. Larvae of leaf miners have dorsoventrally flattened bodies and heads, with a pair of sclerotized mandibles that they use to feed on the epidermal cell layer of their leaf. When observed through a stereomicroscope and lit from below, individual bites can be seen and counted. To construct a thermal performance curve for feeding, in 2019 we measured bite rates of 41 larvae exposed to series of fixed temperatures. Mined leaves were detached from their tree and returned immediately to a nearby shed in which we had set up a stereomicroscope (Nikon SMZ1500). Leaves were mounted one at a time in one of the Sensorspace heater boxes (described above), and ramped from room temperature through a series of higher temperatures. The lowest possible temperatures were set by the shed temperature, which varied by day and warmed throughout any given day (10 – 20 °C). At a given temperature, larvae were given several minutes to adjust, then bites were counted for 5 minutes. The temperature was then increased by ~ 5 °C and the process repeated. Bite rate (per second) was estimated as number of bites divided by the total number of seconds of observation. For individual larvae, we measured bite rate at 2 – 6 temperatures (mean

3.95), and the highest temperatures were between 35 and 42 °C. Larval mass was subsequently estimated from mine size as described above.

Analyses.

All analyses were done using scripts written in R (v 3.6.1) (R Development Core Team 2019). Individual analyses are described in greater detail below. Many experiments, however, involved repeated measurements of individual larvae over time or at different temperatures. In these cases, we generally accounted for the non-independence of data using mixed effects models implemented in the R package *nlme* (Pinheiro et al. 2019). Data from the incubator growth required additional modeling approaches (described below and in Appendix S1: Section S1) to account for effects of larval molting on patterns of growth.

Modeling current and future thermal risks and opportunities.

The data and models described above provide information on (i) spatial and temporal patterns of temperature variation that larvae are likely to experience in the wild and (ii) thermal performance curves for larvae, including upper limits for performance and survival. We used this information to estimate both current risks to larvae and future risks and opportunities arising from +3 °C of warming during climate change.

To estimate risks, we first extracted empirical distributions of T_{excess} ($T_{leaf} – T_{air}$) from shaded and sunny leaves separately (see Figure S6). We then superimposed the extra warming generated by the mines (+ 1 °C for shaded leaves, + 1.6 °C for sunny leaves, see Results) and applied these distributions of temperature differences to long-term time series of air temperature. In particular, we leveraged a long-term data set (back to 1999) from a weather station in Condon, MT (a RAWS station on the Western Regional Climate Center network, 3.8 km WNW of the field site, 1126 m elevation), for which mean daily air temperatures and maximum daily temperatures were highly correlated with those we measured at MPG North during the years 2017 - 2019 (Appendix S1: Figure S7). Using these relationships, we estimated patterns of thermal stress during May – August from 1999 – 2020. For each day of each year during the focal period, we estimated the proportion of mines that exceeded our estimated values of CT_{MAX} and ULT using both measured values and with +3 °C of warming.

To evaluate the magnitude of potential positive effects of warming, we used our fitted thermal performance curve for growth to simulate mean larval growth rates over a 4-week period from mid-May to mid-June in 2017 - 2019. We then reran the simulations with +3 °C of warming added to each temperature trace. Because the model is stochastic, we obtained distributions of growth rates from 10,000 model simulations.

Results

Spatial and temporal variability in leaf temperature.

During the daytime, peak illuminances outside the shades (unmanipulated leaves on the sunny side of the tree) were about 3 – 5× higher than the illuminances under the shades (20,000 – 50,000 lux versus < 10,000 lux) (see Appendix S1: Figure S2). Over the course of the two 3-day experimental periods, we measured leaf temperatures of 20 pairs of shaded and sun-exposed leaves. In most pairs, leaf temperatures were similar during late evening, night, and early morning (in some cases, shaded leaves were slightly warmer at night, probably because they were shielded from exposure to the clear night sky). During the day, the sun-exposed leaf of each pair was often similar in temperature to the shaded leaf, but with distinct, rapid spikes up to temperatures 3 – 8 °C warmer than the shaded leaves (an example shown in Figure 3A). This represents the contribution of direct sunlight to leaf temperature, with additional variability imposed by passing clouds, changes in wind speed, and positioning of focal leaves in relation to nearby leaves and stems. The term 'sun-exposed' leaf refers to its experimental status as 'not shaded,' which does not mean that it was necessarily fully illuminated by the sun. Indeed, because aspen canopies are so complex, 'sun-exposed' leaves were often shaded by other leaves in the canopy while being illuminated intermittently by sunflecks.

To visualize the entire data set, we constructed density plots for each temperature trace, and then estimated the mean and error (standard errors) within each treatment (sun or shade) (Figure 3B, C). The densities of leaf temperatures from the sunny treatment showed an extended right tail, corresponding to the short periods of elevated temperatures.

Environmental drivers of variation in leaf temperature.

We analyzed logged leaf temperatures in relation to data on air temperature, global horizontal solar radiation (direct plus diffuse), and wind speed collected from the nearby weather station. Because nighttime leaf temperatures clearly were driven by air temperature (see Figure 3A), we focused these subsequent analyses on daytime temperatures between 9 am and 4 pm during the periods of the two sun/shade experiments (May 22 – 28, 2018).

During the daytime, leaf temperatures increased linearly with air temperature, and, at the highest air temperatures also showed the largest deviations to higher temperatures, reaching in a few instances temperatures that were 10 – 15 °C warmer (Figure 4A). We analyzed these differences using a linear mixed-effects model with air temperature and treatment (sun-exposed or shaded) as main effects plus their interaction, and with the ID of the leaf pair as a random factor. The intra-pair difference between sun-exposed and shaded leaves also showed a significant positive relationship with air temperature ($F_{1,\,3453} = 85.6$, $P < 0.0001$). This likely reflects that the highest air temperatures occurred in mid-afternoon when intense solar radiation and occasional lulls in the wind combined to raise leaf temperatures significantly above local air temperatures, especially for sun-exposed leaves (see Vogel 2009). Finally, a significant number of leaf temperature observations were 1 – 3 °C below observed air temperatures, likely reflecting slight cooling from transpiration by leaves in the shade. In addition, the weather station and the main aspen site were separated by ~500 m. Given the complexity of air flowing over the landscape, it would not be surprising if local air temperatures at the aspen site temporarily fell several degrees below those measured at the station.

Leaf temperature also showed weak patterns in relation to global solar radiation and wind speed (Appendix S1: Figure S3). Basic considerations of heat-exchange (Gates 1980) suggest that both solar radiation and wind speed must influence leaf temperatures interactively. In our data set, however, their influences were small, likely because of complex microspatial effects (shading and intra-canopy patterns of airflow), and because of spatial and temporal correlations among environmental factors.

Leaf temperature as a function of angle to the sun.

Leaf temperatures (N = 7) were assessed on two days, June 5 and June 12, 2020, between 13:30 and 15:00. On June 5, mean air temperature was 22.3 °C (range 21.6 – 23.4), mean maximum wind speed was 5.3 m/s (2.6 – 5.8), and mean global irradiance was 661 W/m^2 (212 – 1138). On June 12, mean air temperature was 26.2 °C (range 25.7 – 26.6), mean maximum wind speed was 4.3 m/s (3.2 – 6.1), and mean global irradiance was 759 W/m^2 (621 – 884). Leaf T_{excess} was highest (2.5 – 6 °C) when the leaf surface was orthogonal to direct solar radiation and decreased linearly to approximately zero as the leaf approached edge-on to the sun (angle of 85°) (Appendix S1: Figure S4). We analyzed these data using a linear mixed-effects model, with leaf ID as a random effect. The effect of leaf angle on T_{excess} was highly significant ($F_{1,20} = 112$, $P < 0.0001$).

Leaf temperature of mined versus unmined tissue.

Infrared imaging revealed that mined tissues were significantly warmer than unmined tissues, with the relative difference depending on level of illumination (Table 1, Figure 5). Overall, leaves were 3.6 °C warmer in the sun than in the shade. In shaded leaves, mines were 1.0 °C warmer than nearby unmined tissues on the same leaf, whereas in sunny leaves, mines were 1.6 °C warmer. Leaves in partial shade showed intermediate values.

To examine whether mining activity on a leaf alters the temperature of nearby unmined tissue, we compared temperatures of unmined tissues from pairs of leaves ($N = 42$ pairs) positioned near one another on the same branch and of which one was mined and the other was not. Although light condition had effects like those observed in Figure 5, there was no difference in temperature between unmined portions of the mined leaf and its pair that was completely unmined ($F_{1,37} = 1.30$, $P = 0.26$). These data suggest that mines and leaf-miner activity do not influence the physiology (e.g., stomatal conductance) of nearby unmined tissues.

Larval size and growth rates calculated from mine areas.

Mine area and larval mass were highly correlated (Figure 6), and initial analyses showed that there was no significant main effect of year or an interaction between year and mine area. We therefore fit a single linear model to the pooled data ($\log_{10}$ larval mass = 0.294 + 0.992 $\log_{10}$

mine area, $R^2 = 0.96$). This relationship was used subsequently to estimate larval mass from images of mine area.

Growth rates of larvae on sun-exposed versus shaded leaves.

From the images made every morning and evening of paired mines in the sun-vs-shade experiment, we extracted mine areas digitally and used the relationship established above (Figure 6) to estimate larval mass. Together with information on times that images were taken, we estimated mass-specific larval growth rates during each half-day period during the three-day experiment (3 evening/nights and 2 days). Preliminary analysis suggested that homoscedasticity was improved by log-transforming both initial mass and growth rates, so log-transformed values were used in all subsequent analyses. In addition, we excluded individuals from further analysis if during particular intervals they effectively did not grow (defined as growth rates less than 5 µg/mg/hour).

Growth rates were highly variable (Figure 7), likely reflecting the combined effects of many unmeasured and uncontrolled factors (leaf-to-leaf variation in nutritional content, secondary chemistry, parasitism, etc.). In addition, larvae go through periodic molts, during which time they do not feed or grow. Because larvae were small and partially obscured under the leaf cuticle, we were unable to determine whether individuals were molting at given imaging times (see analysis below of incubator growth rates for more on the effects of molting on growth estimates). Despite these complications, larvae clearly grew more rapidly during the daytime than at night, but sun-exposed larvae grew no faster than shaded larvae (Table 2).

Upper lethal temperatures.

Upper lethal temperatures (Figure 8) were estimated first by fitting a logistic regression model that depicted survival as a function of mean logged temperature during the 1-hour heat shock. Temperature was a significant predictor of outcome (z-value -3.007, $P < 0.005$), and the estimated LT_{50} (temperature that killed 50% of larvae) was 42.09 ± 0.43 (sem). Clearly, some larvae experiencing lower temperatures also died, probably from other causes like diseases or parasitoids. Alternative sources of mortality, when they are common (as they appear to be at our field site), will have the statistical effect of biasing the estimated LT_{50} downward (see simulations of this effect in Appendix S1: Figure S5). A reasonable bounded estimate of the upper lethal temperature may be the highest recorded temperature at which a larva survived (43.1 °C), and the true ULT thus lies between 42.1 and 43.1 °C.

Thermal performance curves from short-term incubator experiments.

Larval growth rates were measured from change in mine area in constant-temperature incubators over 8 hours, using established relationships between mine area and larval mass (see Figure 6). Using this approach, growth rates and feeding rates (measured as change in mine area per unit time) are effectively equivalent. At any given temperature, growth rates were highly variable, but with a clear upper limit to growth (Figure 9). The highest observed growth rate occurred at 30 °C, and growth rates were similarly high between 25 and 35 °C.

Even when accounting for initial body mass, the data were multimodal, with one of the modes near zero across all temperature treatments (Figure 9). A likely explanation for the mode near zero is that a fraction of the population was molting – and therefore not leaf mining – during some or all of the 8-hour measurement period. The other mode was likely generated by individuals that were not molting during this period and thus mining normally.

Because larvae were very small, we could not determine the individual states (molting or not molting) during the measurement period. Nevertheless, it is straightforward to account for multiple states using a mixture model, which assumes measurements are drawn from two or more data-generating processes and for which inferences about these processes are possible even when it is not known *a priori* which process generated which measurement. In our case, we assumed there were two processes: (1) molting, in which larvae are not consuming leaf tissue (i.e., performance equals zero, regardless of temperature) and (2) non-molting, in which larvae are consuming tissue and the amount mined is a non-negative function of temperature (i.e., thermal performance function). For added realism, we also assumed that larvae beginning the measurement period in one state had a chance of switching to the other. Based on these assumptions, we formed a likelihood function and used numerical optimization to find the parameters of the mixture model (including the thermal performance function) that maximized the likelihood. Further details on the mixture model are in Appendix S1: Section S1.

Thermal performance curves for feeding in acutely imposed temperatures.

Preliminary analyses indicated that bite rate was positively related to larval mass (Figure 10A; bites per second = 0.148 + 0.589 × $\log_{10}$ larva mass, $R^2 = 0.73$, $P_{1,36} < 0.0001$). To account for this effect, we divided estimates of bite rate by $\log_{10}$ of body mass and plotted mass-specific bite rate as a function of temperature (Figure 10B). Larval feeding rate increased from the lowest temperatures (10 – 15 °C) up to a broad maximum between 20 and 32 °C, before declining steeply at temperatures of 35 °C and above (Figure 10B). The two smallest larvae in the data set (masses of 1.96 and 2.20 μg) had anomalously high estimated bite rates, probably because we divided by very small $\log_{10}$ values of mass. These two larvae were excluded as outliers from the curve fitting described below.

To characterize the overall pattern of performance by temperature, we fit a four-parameter version of the equation used by Deutsch et al. (Deutsch et al. 2008):

$$P = \{z_{max}\left[exp\ exp\left\{-\left(\frac{T-T_{opt}}{2\sigma}\right)^2\right\}\right] \quad for\ T \le T_{opt} \quad z_{max}\left[1-\left(\frac{T-T_{opt}}{T_{opt}-CT_{max}}\right)^2\right] for\ T > T_{opt}$$

where z_{max} is the maximum performance, T_{OPT} is the temperature giving the highest performance, σ characterizes the width of the Gaussian rise from lower temperatures toward T_{OPT}, and CT_{MAX} identifies the temperature above T_{OPT} at which performance goes to zero. We fit the equation using a non-linear mixed-effects approach implemented in the R package *nlme*, with larval ID as a random effect within z_{max}. The fit identified z_{max} as 0.66 (95% CI 0.59 – 0.74), T_{OPT} as 25.5 °C (95% CI 22.6 – 28.4), σ as 7.77 (95% CI 3.76 – 11.78), and CT_{MAX} as 39.9 °C (95% CI 38.5 – 41.3).

Modeling current and future thermal risks to leaf miners.

Analyses of long-term records of air temperature (1999 – 2020) indicate that mine temperatures over the past several decades have rarely surpassed high temperature thresholds (CT_{MAX} = 39.9 °C and ULT = 42.6 °C) during the main larval growth period, from mid-May to mid-June (Figure 11). Future climate warming, however, will result in significantly more days on which mine temperatures exceed larval CT_{MAX}, and a few additional days on which they exceed ULT. Our analysis showed that, during this period, there were 1 - 14 additional days per year in which high-temperature thresholds were exceeded (average of 6). From mid-June to the end of July, high temperatures thresholds were surpassed much more frequently, and on some days more than 50% of mine temperatures exceed CT_{MAX}. Late season risks are magnified even more by 3 °C of future warming, with 100% of mine temperatures predicted to exceed CT_{MAX} on some days and up to 50% of mines exceeding ULT. During this period, there were 2 – 16 additional days per year in which high-temperature thresholds were exceeded (average of 8). These seasonal patterns may explain our observations (unpublished) that leaf miner pupae, which construct pupation chambers on leaves in June and that persist through July, have higher ULT than do larvae.

Warmer springs will also accelerate rates of feeding and growth. On average, leaf consumption in 2017 - 2019 was 34% higher under the warming scenario (Figure 12). Future leaf temperatures will depend on many factors, including patterns of cloud cover and hydrological cycles – e.g., more frequent or severe droughts may reduce stomatal opening and rates of transpiration, providing less evaporative cooling to leaves. Regardless, these simulations suggest that rates of feeding will rise significantly, with associated increases in rates of larval growth and earlier pupation.

Discussion

Small terrestrial ectotherms inhabit microclimates in which temporal and spatial thermal variation can be quite different from climatic conditions at larger scales. For these organisms, the partial decoupling of micro- from macroclimate complicates the problem of predicting potential effects of climate change. Progress on these questions has been made in a variety of ecosystems – notably, for invertebrates in rocky intertidal communities (e.g., (Denny et al. 2011; Denny, Miller, and Harley 2006), ectothermic vertebrates in deserts (e.g., (Parlin, Schaeffer, and Jezkova 2020; Sears et al. 2016), and plants in the understory of forests (Zellweger et al. 2020). In addition, the macroecological and evolutionary consequences of microclimatic diversity and behavioral thermoregulation have begun to receive significant attention (Kearney, Shine, and Porter 2009; Sunday et al. 2014).

Using a combination of lab- and field-based approaches, we examined the thermal ecology of an important plant-herbivore interaction. Aspen is the most broadly distributed tree species in North America (Little 1971), occurring from Mexico to Alaska and across boreal Canada. In this range, aspens play ecologically diverse roles (Mueggler 1988), support a broad diversity of insect herbivores (Bailey and Whitham 2002), and employ a diverse set of secondary compounds as defenses, especially phenolic glycosides and condensed tannins (Lindroth and St. Clair 2013). Aspen leaf miners are only one of many Lepidoptera that attack aspen, but they occur widely throughout the range of aspens (Condrashoff 1964) and during outbreaks can reach high densities, damage leaves extensively, and reduce tree growth rates (Wagner et al. 2008). They thus represent a case study that can be leveraged for insight into the thermal experiences of other aspen-associated insects across the range of aspens. In this study, we integrated information on temporal and spatial patterns of temperature variation in aspen leaves with information on thermal performance curves and thermal limits of aspen leaf miners. Collectively, these data and models allow us to predict how much larval performance may shift in the future and the frequencies with which leaf miners approach or exceed their thermal limits in current and future climates.

Temporal and spatial patterns of temperature variation within aspen canopies at scales relevant to leaf miners.

Leaf temperatures varied diurnally from ~5 °C at night to 20 – 30 °C during the day, largely following diurnal variation in air temperature (see also Kingsolver, 2000). During the day, however, leaves showed occasional brief excursions to temperatures of 3 - 8 °C above air temperature. Similar or larger excess leaf temperatures have been observed in other species (Pincebourde et al. 2007; Singsaas et al. 1999; Young and Smith 1979), including *Populus tremula* and hybrids between *P. tremula* and *P. tremuloides* (Hüve et al. 2019). These temperature excesses reflect that leaves are small, with little heat storage but large energy fluxes through the component pathways of the heat budget—primarily radiation, convection (sensible heat), and evaporation (latent heat)—such that some combinations of conditions result in rapidly rising leaf temperatures (Hüve et al. 2019; Vogel 2009). In particular, leaves facing the sun (high incoming solar radiation) in conditions of little or no wind (small convective losses to the air) and with low rates of transpiration (evaporative cooling) can reach temperatures that are high enough to damage leaf tissues or to stress or kill insects living in or on the leaves (Hüve et al. 2019; Pincebourde and Casas 2019; Singsaas et al. 1999).

In aspens, the effects of solar radiation were obscured by a suite of competing processes. In the sun-shade experiment, sunny leaves showed frequent short excursions to temperatures up to 8 °C above ambient air temperature (Figure 3), and leaf temperatures rose higher (Appendix S1: Figure S4) when face-on to the sun compared to other orientations (Medina, Sobrado, and Herrera 1978). The overall distributions of leaf temperatures, however, were similar for experimentally unshaded and shaded leaves (Figure 3). Second, compared to other factors, global radiation did not strongly predict leaf temperatures or temperature differences between unshaded and shaded leaves within a pair (Appendix S1: Figure S3). These (non)effects reflect the complexity of leaves in their natural orientation – often shaded by nearby stems and leaves even when in the 'unshaded' treatment, and even when illuminated they often were oriented so that the leaf face was far from orthogonal to the sun.

A key component of leaf heat budgets is transpiration, which cools leaves by carrying away the latent heat of evaporation. Aspens have relatively high potential rates of transpiration, as measured by canopy conductance estimated from eddy co-variance (Bernier et al. 2006; Blanken et al. 1997) and sap-flow techniques (Hogg and Hurdle 1997; Loranty et al. 2008). Realized conductance in aspens, however, depends on light levels, vapor pressure deficit, and drought status. In particular, stomatal conductance rises linearly with incoming solar radiation (Bernier et al. 2006). In addition, transpiration rate rises linearly with vapor pressure deficits between 0 and 1 kPa and then stabilizes at nearly constant values at higher vapor pressure deficits (Hogg and Hurdle 1997; Hogg et al. 2000)—implying that stomatal conductance declines at the high vapor pressure deficits occurring on hot, dry days. This implies further that transpiration does not contribute increasingly to cooling aspen leaves at the highest temperatures (Dong et al. 2017). Rather, progressive stomatal closure at high temperatures should contribute to further warming. Finally, stomatal conductance and rates of transpiration are positively related to soil water content (Bernier et al. 2006), suggesting that leaf temperatures should cool less from transpiration in drier sites or during droughts. Experimentally, this effect has been observed directly in the European aspen (*P. tremula*) and in hybrids between *P. tremula* and *P. tremuloides* (Hüve et al. 2019). In this study, leaves of drought-stressed *P. tremula* reached maximum temperatures that were on average 8 °C above air temperature (with extremes up to 15 °C greater). Leaf temperatures of potted hybrid plants subjected to experimental drought stress for two weeks reached leaf temperatures up to 20 °C greater than air temperature (maximum leaf temperatures of 44 - 45 °C), with the greatest increases on sunny, calm days.

For leaf miners, a final factor contributing to variation in temperature is the mine itself. On average, mines illuminated by direct sunlight were 1.6 °C warmer than adjacent leaf tissues

(Figure 5), but the temperatures of unmined tissues on a mine-containing leaf were no different than temperatures of unmined leaves. These patterns indicate that mines do not have systematic effects on nearby unmined tissues. Two mechanisms may contribute to local mine heating – changes in how mines interact with radiation and changes in stomatal conductance of mined tissues. In a detailed study of the biophysics of mine temperature of the apple leaf miner (*Phyllonorycter blancardella*) on apple leaves (*Malus communis*), Pincebourde & Casas (2006) found that, compared to unmined tissues, mined tissues absorbed greater proportions of incoming long-wave radiation and exhibited greater stomatal closure at high levels of incoming solar radiation. Together, these effects led mines to warm significantly, and the authors' biophysical model predicted mine temperatures up to 5 °C above temperatures of nearby unmined tissues. This deviation is larger than the mean deviation (1.6 °C) we observed in our system under field conditions, which probably reflects differences in mine and leaf morphologies between the two systems. For aspens, Wagner et al. (2020) showed that leaves mined abaxially (but not adaxially) by *P. populiella* also exhibit stomatal closure. They did not measure energy budgets of mined versus unmined leaves—but, all else being equal, stomatal closure should lead to mine warming.

Current and future thermal performance and thermal risks.

A fundamental, non-thermal risk for leaf miners is the decline of aspens in the Intermountain West. Aspens have declined gradually through the past century with additional diebacks in recent years (Rehfeldt, Ferguson, and Crookston 2009). The causes are diverse but include changes in patterns of fire, ungulate browsing, competition with conifers, snowpack, drought, and temperature (Anderegg et al. 2013; Coop et al. 2014; Kretchun et al. 2020; Rogers, Eisenberg, and St. Clair 2013; Rogers et al. 2014; Seager, Eisenberg, and St. Clair 2013; Shinneman et al. 2013; Yang et al. 2015). A number of studies now predict that declines will accelerate as climate change deepens (Anderegg et al. 2013; Rehfeldt, Ferguson, and Crookston 2009). For example, a bioclimatic niche model of aspens in western North America predicts that populations will contract over the remainder of the century due to shifts in patterns of moisture availability interacting with rising temperatures (Rehfeldt, Ferguson, and Crookston 2009). For aspen stands that persist, however, data from this study provide insight into how changing climates may alter the thermal performance of leaf miners. The data suggest two main conclusions.

First, future warming will accelerate rates of larval feeding and growth and likely will advance the phenology of egg-to-larva and larva-to-pupa transitions. Adult females of *P. populiella* are active early in spring, emerging from protected overwintering sites in the leaf litter to mate and lay eggs as leaves are flushing (Condrashoff 1964). A key challenge for eggs and larvae in early spring is inadequate heat. Larvae spend approximately half of their time at night, during which temperatures in our study varied between 3 and 13 °C, low enough to strongly depress rates of feeding (Figure 10) and growth (Figures 7, 9) (Kingsolver 2000). Leaf temperatures during daytime were higher but still fell within the range of 15 – 30 °C, which is below or near temperatures supporting maximal rates (25 – 32 °C). The highest measured leaf temperatures were ~ 35 °C (including measurements from two other springs, in 2018 and 2020), which are nearing temperatures that depress feeding and growth but still are far from the measured ULT of 42 - 43 °C. In the moderate conditions prevailing during our experiments, which were similar to May conditions in most years, a few degrees of warming may thus significantly improve performance (see Figures 9, 10, 12). The fitted two-state stochastic model (see Figure 12) suggests that +3 °C of warming will increase rates of feeding and growth by 34%.

Second, at the same time, future, warmer temperatures will also increase the probability that mine temperatures rise above CT_{MAX} or ULT. We estimated the proportion of mines exceeding critical thresholds based on the empirical relationships observed among leaf, mine, and air temperatures at MPG North (Figure 11). During the main larval growth period at our study site (mid-May to mid-June), the proportions of leaves exceeding CT_{MAX} were very low for sun-exposed leaves and even lower for shaded leaves; proportions exceeding ULT were exceedingly low for both leaf types. Under the +3 °C warming scenario, however, probabilities of exceeding CT_{MAX} were substantially higher (above 5% for shaded leaves and 20% for sunny leaves in some years). Likewise, estimated probabilities of exceeding ULT in sunny leaves increased from virtually zero without warming to 5 – 10% in some years.

After the main larval growth period, which ends in mid-June, the probability that mine temperatures exceed larval thermal thresholds rises steeply in current conditions and to even higher levels with warming. These patterns suggest strong constraints on the timing of oviposition and growth: females must oviposit early enough in May, or larvae must growth fast enough, to have reached the end of the growth phase by mid-June. Our data suggest that spring warming will contribute to the latter effect: by accelerating feeding and growth, future warming likely will result in earlier pupation, all else being equal. Warming may also drive earlier oviposition. Condrashoff (1964), for example, showed that adult activity, including mating and oviposition, depended on temperature and occurred most frequently at temperatures between 10 and 15 °C. If these thresholds are reached earlier in spring, oviposition may also start earlier. The timing of vernal leaf-flushing, however, appears to be relatively temperature-insensitive (Creed et al. 2015), suggesting potential future mismatches between adult activity and initial leaf availability.

Finally, will climate-driven shifts in insect herbivory contribute to aspen declines? The answer will depend on the net effects of the temperature-dependent influences outlined above. Higher temperatures may indeed support higher insect performance and survival, larger population sizes, and greater impacts on local aspen populations, with minimal additional mortality from thermal stress. Alternatively, once mine temperatures regularly approach or exceed CT_{MAX} and ULT, climate warming likely will depress population sizes of miners and reduce the damage they cause. We suspect that the former scenario is more likely in the coming decades (more damage from accelerated larval growth), as even +3 °C of warming will not kill more than 50% of the population in most years during the main larval growth period. In addition, warmer nightimes during climate change are likely to increase rates of feeding—because nighttime temperatures lie below the optimal temperature and therefore well below CT_{MAX} (Barton and Schmitz 2018), suggesting a net positive impact of warming. These conclusions, however, stem from our data on the larval phase, which is just one of four life stages -- and population responses may depend on climate effects in other stages (Kingsolver et al. 2011; Williams, Henry, and Sinclair 2015). Risks to pupae and adults, for example, include reaching ULT during high mid-summer temperatures and the energetic demands of prolonged summertime exposure to elevated temperatures. Moreover, climate change may drive phenological mismatches between aspens, leaf miners, and the parasitoid wasps that are one of their major sources of mortality (Shah et al. 2020, Shah et al. unpublished).

Extensions: thermal opportunities and risks across time and space.

Our conclusions about thermal opportunities and risks reflect data collected at a single site in western Montana. How significant are opportunities and risks in other places and over longer time scales, and how will climate change alter their balance? Potential approaches to answering this question include using biophysical models of leaf and mine temperature (for an example, see (Pincebourde and Casas 2006) and the *tealeaves* package in R (Muir 2019)) or statistical models that estimate the risk of climatic coincidences that generate unusually high leaf and mine temperatures (Denny et al. 2009; Vogel 2009) – e.g., high air temperatures, intense solar radiation, and very low wind speeds. At present, we lack the requisite biophysical details and long-term climatic records to support such models. Nevertheless, elucidating responses at other sites will require fine-scale climatic data (increasingly available) and information on variation in the heat budgets of aspen leaves and larval thermal performance across their respective geographic ranges. A tractable approach to this problem would be to use a space-for-time approach – to examine larval performance in aspen stands distributed across strong spatial gradients in abiotic conditions, i.e, across latitudinal gradients within the range of aspens or across within-drainage elevational gradients in the Rocky Mountains.

Acknowledgments. This work was supported by the MPG Ranch and The University of Montana. We thank Rachel Bingham, Jackson Birrell, Ben Borhegyi, Markus Boyer, Dominic Cuellar, Rachel Dixson, Phil Douchinsky, James Frakes, Emily Hamant, Tylor Keely, Priya Keller, Sean Kellogg, Mark Randolph, Brenna Shea, and Reed Traynor for help in the field and lab, and Jérôme Casas for discussions on leaf miner ecophysiology.

Funding. This work was supported by several grants from MPG Ranch to HAW.

Conflict of Interest Statement. The authors declare no conflicts of interest.

Literature cited

Aldea, Mihai, Jason G Hamilton, Joseph P Resti, Arthur R Zangerl, May Berenbaum, and Evan H DeLucia. 2005. "Indirect Effects of Insect Herbivory on Leaf Gas Exchange in Soybean ." *Plant, Cell and Environment* 28: 402–11.

Anderegg, William R.L., Lenka Plavcová, Leander D.L. Anderegg, Uwe G. Hacke, Joseph A. Berry, and Christopher B. Field. 2013. "Drought's Legacy: Multiyear Hydraulic Deterioration Underlies Widespread Aspen Forest Die-off and Portends Increased Future Risk." *Global Change Biology* 19 (4): 1188–96. https://doi.org/10.1111/gcb.12100.

Bailey, Joseph K., and Thomas G. Whitham. 2002. "Interactions among Fire, Aspen, and Elk Affect Insect Diversity: Reversal of a Community Response." *Ecology* 83 (6): 1701–12. https://doi.org/10.1890/0012-9658(2002)083[1701:IAFAAE]2.0.CO;2.

Bernier, P. Y., P. Bartlett, T. A. Black, A. Barr, N. Kljun, and J. H. McCaughey. 2006. "Drought Constraints on Transpiration and Canopy Conductance in Mature Aspen and Jack Pine Stands." *Agricultural and Forest Meteorology* 140 (1–4): 64–78. https://doi.org/10.1016/j.agrformet.2006.03.019.

Blanken, P. D., T. A. Black, P. C. Yang, H. H. Neumann, Z. Nesic, R. Staebler, G. Den Hartog, M. D. Novak, and X. Lee. 1997. "Energy Balance and Canopy Conductance of a Boreal Aspen Forest: Partitioning Overstory and Understory Components." *Journal of Geophysical Research Atmospheres* 102 (24): 28915–27. https://doi.org/10.1029/97jd00193.

Bogert, C.M. 1949. "Thermoregulation in Reptiles: A Factor in Evolution." *Evolution* 3: 195–211.

Caillon, Robin, Christelle Suppo, J Casas, H A Woods, and Sylvain Pincebourde. 2014. "Warming Decreases Thermal Heterogeneity of Leaf Surfaces: Implications for Behavioural Thermoregulation by Arthropods." *Functional Ecology* 28 (6): 1449–58. https://doi.org/10.1111/1365-2435.12288.

Campbell, G.S., and J.M. Norman. 1998. *An Introduction to Environmental Biophysics*. Springer.

Cockfield, S D, and D A Potter. 1986. "Interaction of Euonymus Scale (Homoptera: Diaspididae) Feeding Damage and Severe Water Stress on Leaf Abscission and Growth of Euonymus Fortunei." *Oecologia* 71 (86): 41–46.

Condrashoff, S. F. 1964. "Bionomics of the Aspen Leaf Miner, Phyllocnistis Populiella Cham. (Lepidoptera: Gracillariidae)." *The Canadian Entomologist*. https://doi.org/10.4039/Ent96857-6.

Coop, Jonathan D., Kristin J. Barker, Adrian D. Knight, and Joseph S. Pecharich. 2014. "Aspen (Populus Tremuloides) Stand Dynamics and Understory Plant Community Changes over 46years near Crested Butte, Colorado, USA." *Forest Ecology and Management* 318: 1–12. https://doi.org/10.1016/j.foreco.2014.01.019.

Creed, I. F., T. Hwang, B. Lutz, and D. Way. 2015. "Climate Warming Causes Intensification of the Hydrological Cycle, Resulting in Changes to the Vernal and Autumnal Windows in a Northern Temperate Forest." *Hydrological Processes* 29 (16): 3519–34. https://doi.org/10.1002/hyp.10450.

Denny, Mark W., W. Wesley Dowd, Lisa Bilir, and Katharine J. Mach. 2011. "Spreading the Risk: Small-Scale Body Temperature Variation among Intertidal Organisms and Its Implications for Species Persistence." *Journal of Experimental Marine Biology and Ecology* 400 (1–2): 175–90. https://doi.org/10.1016/j.jembe.2011.02.006.

Denny, Mark W., L. J H Hunt, Luke P. Miller, and C. D G Harley. 2009. "On the Prediction of Extreme Ecological Events." *Ecological Monographs* 79 (3): 397–421. https://doi.org/10.1890/08-0579.1.

Denny, Mark W., Luke P. Miller, and Christopher D.G. Harley. 2006. "Thermal Stress on Intertidal Limpets: Long-Term Hindcasts and Lethal Limits." *Journal of Experimental Biology* 209 (13): 2420–31. https://doi.org/10.1242/jeb.02258.

Deutsch, Curtis A., Joshua J. Tewksbury, Raymond B. Huey, Kimberly S. Sheldon, Cameron K. Ghalambor, David C. Haak, and Paul R. Martin. 2008. "Impacts of Climate Warming on Terrestrial Ectotherms across Latitude." *Proceedings of the National Academy of Sciences of the United States of America* 105 (18): 6668–72. https://doi.org/10.1073/pnas.0709472105.

Dong, N., I. C. Prentice, S. P. Harrison, Q. H. Song, and Y. P. Zhang. 2017. "Biophysical Homoeostasis of Leaf Temperature: A Neglected Process for Vegetation and Land-Surface Modelling." *Global Ecology and Biogeography*, 2017. https://doi.org/10.1111/geb.12614.

Faye, E., O. Dangles, and S. Pincebourde. 2016. "Distance Makes the Difference in Thermography for Ecological Studies." *Journal of Thermal Biology* 56: 1–9. https://doi.org/10.1016/j.jtherbio.2015.11.011.

Faye, E., F. Rebaudo, C. Carpio, M. Herrera, and O. Dangles. 2017. "Does Heterogeneity in

Crop Canopy Microclimates Matter for Pests? Evidence from Aerial High-Resolution Thermography." *Agriculture, Ecosystems and Environment* 246: 124–33. https://doi.org/10.1016/j.agee.2017.05.027.

Gates, D. M. 1980. *Biophysical Ecology*. New York: Springer-Verlag.

Gates, D M. 1968. "Transpiration and Leaf Temperature." *Annual Review of Plant Physiology*. https://doi.org/10.1146/annurev.pp.19.060168.001235.

Helmuth, Brian, BR Bernardo R Broitman, Carol A Blanchette, Sarah Gilman, Patricia Halpin, Christopher D G CDG Harley, Michael J MJ O'Donnell, GE Gretchen E Hofmann, Bruce Menge, and Denise Strickland. 2006. "Mosaic Patterns of Thermal Stress in the Rocky Intertidal Zone: Implications for Climate Change." *Ecological Monographs* 76 (4): 461–79. https://doi.org/10.1890/0012-9615(2006)076[0461:MPOTSI]2.0.CO;2.

Henson, W R. 1958. "The Effects of Radiation on the Habitat Temperatures of Some Poplar-Inhabiting Insects." *Canadian Journal of Zoology* 36 (453): 463–78.

Hogg, E. H., and P. A. Hurdle. 1997. "Sap Flow in Trembling Aspen: Implications for Stomatal Responses to Vapor Pressure Deficit." *Tree Physiology* 17 (8–9): 501–9. https://doi.org/10.1093/treephys/17.8-9.501.

Hogg, E. H., B. Saugier, J. Y. Pontailler, T. A. Black, W. Chen, P. A. Hurdle, and A. Wu. 2000. "Responses of Trembling Aspen and Hazelnut to Vapor Pressure Deficit in a Boreal Deciduous Forest." *Tree Physiology* 20 (11): 725–34. https://doi.org/10.1093/treephys/20.11.725.

Huey, Raymond B., Paul E. Hertz, and B. Sinervo. 2003. "Behavioral Drive versus Behavioral

Inertia in Evolution: A Null Model Approach.” *American Naturalist* 161 (3): 357–66. https://doi.org/10.1086/346135.

Hüve, Katja, Irina Bichele, Hedi Kaldmäe, Bahtijor Rasulov, Fernando Valladares, and Ülo Niinemets. 2019. “Responses of Aspen Leaves to Heatflecks: Both Damaging and Non-Damaging Rapid Temperature Excursions Reduce Photosynthesis.” *Plants* 8 (6): 145. https://doi.org/10.3390/plants8060145.

Jones, H. G. 1999. “Use of Thermography for Quantitative Studies of Spatial and Temporal Variation of Stomatal Conductance over Leaf Surfaces.” *Plant, Cell and Environment* 22 (9): 1043–55. https://doi.org/10.1046/j.1365-3040.1999.00468.x.

Kaspari, Michael, Natalie A. Clay, Jane Lucas, Stephen P. Yanoviak, and Adam Kay. 2015. “Thermal Adaptation Generates a Diversity of Thermal Limits in a Rainforest Ant Community.” *Global Change Biology* 21 (3): 1092–1102. https://doi.org/10.1111/gcb.12750.

Kearney, Michael, Richard Shine, and W. P. Porter. 2009. “The Potential for Behavioral Thermoregulation to Buffer ‘Cold-Blooded’ Animals against Climate Warming.” *Proc Natl Acad Sci U S A* 106 (10): 3835–40. http://www.pnas.org/content/106/10/3835.short.

Kingsolver, J.G. 1979. “Thermal and Hydric Aspects of Environmental Heterogeneity in the Pitcher Plant Mosquito.” *Ecological Monographs* 49 (4): 357–76.

Kingsolver, Joel G. 2000. “Feeding, Growth, and the Thermal Environment of Cabbage White Caterpillars, Pieris Rapae L.” *Physiological and Biochemical Zoology* 73 (5): 621–28. https://doi.org/10.1086/317758.

Kingsolver, Joel G., H. Arthur Woods, Lauren B. Buckley, Kristen A. Potter, Heidi J. MacLean, and Jessica K. Higgins. 2011. "Complex Life Cycles and the Responses of Insects to Climate Change." *Integrative and Comparative Biology* 51 (5): 719–32. https://doi.org/10.1093/icb/icr015.

Kretchun, Alec M., Robert M. Scheller, Douglas J. Shinneman, Benjamin Soderquist, Kaitlin Maguire, Timothy E. Link, and Eva K. Strand. 2020. "Long Term Persistence of Aspen in Snowdrift-Dependent Ecosystems." *Forest Ecology and Management* 462 (January): 118005. https://doi.org/10.1016/j.foreco.2020.118005.

Leuzinger, Sebastian, and Christian Körner. 2007. "Tree Species Diversity Affects Canopy Leaf Temperatures in a Mature Temperate Forest." *Agricultural and Forest Meteorology* 146 (1–2): 29–37. https://doi.org/10.1016/j.agrformet.2007.05.007.

Lill, John T, and Robert J Marquis. 2007. "Microhabitat Manipulation: Ecosystem Engineering By Shelter-Building Insects." In *Ecosystem Engineers: Plants to Protists*, 107–38.

Linacre, E. T. 1964. "A Note on a Feature of Leaf and Air Temperatures." *Agricultural Meteorology* 1: 66–72.

———. 1967. "Further Notes on a Feature of Leaf and Air Temperatures." *Theoretical and Applied Climatology* 15: 422–36.

Lindroth, Richard L., and Samuel B. St. Clair. 2013. "Adaptations of Quaking Aspen (Populus Tremuloides Michx.) for Defense against Herbivores." *Forest Ecology and Management* 299: 14–21. https://doi.org/10.1016/j.foreco.2012.11.018.

Little, Elbert L. 1971. *Atlas of United States Trees. Volume 1: Conifers and Important*

Hardwoods. Miscellaneous Publication 1146. USDA Forest Service. Atlas of United States Trees.

Loranty, Michael M., D. Scott Mackay, Brent E. Ewers, Jonathan D. Adelman, and Eric L. Kruger. 2008. "Environmental Drivers of Spatial Variation in Whole-Tree Transpiration in an Aspen-Dominated Upland-to-Wetland Forest Gradient." *Water Resources Research* 44 (2): 1–15. https://doi.org/10.1029/2007WR006272.

Ma, Chun Sen, Gang Ma, and Sylvain Pincebourde. 2021. "Survive a Warming Climate: Insect Responses to Extreme High Temperatures." *Annual Review of Entomology* 66: 163–84. https://doi.org/10.1146/annurev-ento-041520-074454.

Medina, E., M. Sobrado, and R. Herrera. 1978. "Significance of Leaf Orientation for Leaf Temperature in an Amazonian Sclerophyll Vegetation." *Radiation and Environmental Biophysics* 15 (2): 131–40. https://doi.org/10.1007/BF01323262.

Meisel, J. E. 2006. "Thermal Ecology of the Neotropical Army Ant." *Ecological Applications* 16 (3): 913–22.

Michaletz, Sean T., Michael D. Weiser, Nate G. McDowell, Jizhong Zhou, Michael Kaspari, Brent R. Helliker, and Brian J. Enquist. 2016. "The Energetic and Carbon Economic Origins of Leaf Thermoregulation." *Nature Plants*. https://doi.org/10.1038/nplants.2016.129.

Michaletz, Sean T., Michael D. Weiser, Jizhong Zhou, Michael Kaspari, Brent R. Helliker, and Brian J. Enquist. 2015. "Plant Thermoregulation: Energetics, Trait-Environment Interactions, and Carbon Economics." *Trends in Ecology and Evolution* 30 (12): 714–24. https://doi.org/10.1016/j.tree.2015.09.006.

Miller, Benjamin D., Kelsey R. Carter, Sasha C. Reed, Tana E. Wood, and Molly A. Cavaleri. 2021. “Only Sun-Lit Leaves of the Uppermost Canopy Exceed Both Air Temperature and Photosynthetic Thermal Optima in a Wet Tropical Forest.” *Agricultural and Forest Meteorology* 301–302 (July 2020): 108347. https://doi.org/10.1016/j.agrformet.2021.108347.

Mueggler, W. F. 1988. “Aspen Community Types of the Intermountain Region.” *General Technical Report - US Department of Agriculture, Forest Service*. https://doi.org/10.5962/bhl.title.100147.

Muir, C. D. 2019. “Tealeaves: An R Package for Modelling Leaf Temperature Using Energy Budgets.” *AoB PLANTS* 11: plz054.

Muñoz, M M, and B L Bodensteiner. 2019. “Janzen’s Hypothesis Meets the Bogert Effect: Connecting Climate Variation, Thermoregulatory Behavior, and Rates of Physiological Evolution.” *Integrative Organismal Biology* 1 (1): oby002. https://doi.org/10.1093/iob/oby002.

Nobel, P. S. 1999. *Physicochemical & Environmental Plant Physiology*. New York: Academic Press.

Odling-Smee, John, Kevin N. Laland, and M. W. Feldman. 2003. *Niche Construction: The Neglected Process in Evolution*. Princeton University Press.

Oke, T. R. 2002. *Boundary Layer Climates*. London: Routledge.

Parlin, Adam F., Paul J. Schaeffer, and Tereza Jezkova. 2020. “Modelling the Effect of Environmental Temperatures, Microhabitat and Behavioural Thermoregulation on Predicted

Activity Patterns in a Desert Lizard across Its Thermally Diverse Distribution." *Journal of Biogeography*. https://doi.org/10.1111/jbi.13936.

Perez, Timothy M., and Kenneth J. Feeley. 2020. "Photosynthetic Heat Tolerances and Extreme Leaf Temperatures." *Functional Ecology* 34 (11): 2236–45. https://doi.org/10.1111/1365-2435.13658.

Pincebourde, Sylvain, and Jerome Casas. 2006. "Multitrophic Biophysical Budgets: Thermal Ecology of an Intimate Herbivore Insect-Plant Interaction." *Ecological Monographs* 76 (2): 175–94.

Pincebourde, Sylvain, and Jérôme Casas. 2019. "Narrow Safety Margin in the Phyllosphere during Thermal Extremes." *Proceedings of the National Academy of Sciences of the United States of America* 116 (12): 5588–96. https://doi.org/10.1073/pnas.1815828116.

Pincebourde, Sylvain, Michael E. Dillon, and H. Arthur Woods. 2021. "Body Size Determines the Thermal Coupling between Insects and Plant Surfaces." *Functional Ecology*, no. November 2020: 1–13. https://doi.org/10.1111/1365-2435.13801.

Pincebourde, Sylvain, C. C. Murdock, M. Vickers, and M. W. Sears. 2016. "Fine-Scale Microclimatic Variation Can Shape the Responses of Organisms to Global Change in Both Natural and Urban Environments." *Integrative and Comparative Biology* 56: 45–61.

Pincebourde, Sylvain, Herve Sinoquet, Didier Combes, and Jerome Casas. 2007. "Regional Climate Modulates the Canopy Mosaic of Favourable and Risky Microclimates for Insects." *Journal of Animal Ecology* 76 (3): 424–38.

Pincebourde, Sylvain, and Christelle Suppo. 2016. "The Vulnerability of Tropical Ectotherms to

Warming Is Modulated by the Microclimatic Heterogeneity.” *Integrative and Comparative Biology* 56 (1): 85–97. https://doi.org/10.1093/icb/icw014.

Pincebourde, Sylvain, and H. Arthur Woods. 2012. “Climate Uncertainty on Leaf Surfaces: The Biophysics of Leaf Microclimates and Their Consequences for Leaf-Dwelling Organisms.” *Functional Ecology* 26 (May): 844–53. https://doi.org/10.1111/j.1365-2435.2012.02013.x.

———. 2020. “There Is Plenty of Room at the Bottom: Microclimates Drive Insect Vulnerability to Climate Change.” *Current Opinion in Insect Science* 41: 63–70. https://doi.org/10.1016/j.cois.2020.07.001.

Pinheiro, J, D Bates, S DebRoy, D Sarkar, and R Core Team. 2019. “Nlme: Linear and Nonlinear Mixed Effects Models, R Package Version 3.1-140.”

Potter, Kristen A., Goggy Davidowitz, and H. Arthur Woods. 2009. “Insect Eggs Protected from High Temperatures by Limited Homeothermy of Plant Leaves.” *Journal of Experimental Biology* 212 (Pt 21): 3448–54. http://www.ncbi.nlm.nih.gov/pubmed/19837886.

Potter, Kristen A., H. Arthur Woods, and Sylvain Pincebourde. 2013. “Microclimatic Challenges in Global Change Biology.” *Global Change Biology* 19 (10): 2932–39. https://doi.org/10.1111/gcb.12257.

R Development Core Team. 2019. “R: A Language and Environment for Statistical Computing.” Vienna, Austria: R Foundation for Statistical Computing. http://www.r-project.org.

Rehfeldt, Gerald E., Dennis E. Ferguson, and Nicholas L. Crookston. 2009. “Aspen, Climate, and Sudden Decline in Western USA.” *Forest Ecology and Management* 258 (11): 2353–64. https://doi.org/10.1016/j.foreco.2009.06.005.

Roden, J. S., and R. W. Pearcy. 1993. “The Effect of Flutter on the Temperature of Poplar Leaves and Its Implications for Carbon Gain.” *Plant, Cell & Environment* 16 (5): 571–77. https://doi.org/10.1111/j.1365-3040.1993.tb00905.x.

Rogers, Paul C., Cristina Eisenberg, and Samuel B. St. Clair. 2013. “Resilience in Quaking Aspen: Recent Advances and Future Needs.” *Forest Ecology and Management* 299: 1–5. https://doi.org/10.1016/j.foreco.2012.11.008.

Rogers, Paul C., Simon M. Landhäusser, Bradley D. Pinno, and Ronald J. Ryel. 2014. “A Functional Framework for Improved Management of Western North American Aspen (Populus Tremuloides Michx.).” *Forest Science* 60 (2): 345–59. https://doi.org/10.5849/forsci.12-156.

Saudreau, Marc, Amélie Ezanic, Boris Adam, Robin Caillon, Pascal Walser, and Sylvain Pincebourde. 2017. “Temperature Heterogeneity over Leaf Surfaces: The Contribution of the Lamina Microtopography.” *Plant Cell and Environment* 40 (10): 2174–88. https://doi.org/10.1111/pce.13026.

Scherrer, D, and C Körner. 2010. “Infrared Thermometry of Alpine Landscapes Challenges Climatic Warming Projections.” *Global Change Biology* 16: 2602–13. http://onlinelibrary.wiley.com/doi/10.1111/j.1365-2486.2009.02122.x/full.

Schultz, Tom D. 1998. “The Utilization of Patchy Thermal Microhabitats by the Ectothermic Insect Predator, Cicindela Sexguttata.” *Ecological Entomology* 23 (4): 444–50. https://doi.org/10.1046/j.1365-2311.1998.00154.x.

Schymanski, Stanislaus J., Dani Or, and Maciej Zwieniecki. 2013. “Stomatal Control and Leaf Thermal and Hydraulic Capacitances under Rapid Environmental Fluctuations.” *PLoS ONE*

8 (1). https://doi.org/10.1371/journal.pone.0054231.

Seager, S. Trent, Cristina Eisenberg, and Samuel B. St. Clair. 2013. "Patterns and Consequences of Ungulate Herbivory on Aspen in Western North America." *Forest Ecology and Management* 299: 81–90. https://doi.org/10.1016/j.foreco.2013.02.017.

Sears, Michael W., Michael J. Angilletta, Matthew S. Schuler, Jason Borchert, Katherine F. Dilliplane, Monica Stegman, Travis W. Rusch, and William A. Mitchell. 2016. "Configuration of the Thermal Landscape Determines Thermoregulatory Performance of Ectotherms." *Proceedings of the National Academy of Sciences* 113 (38): 10595–600. https://doi.org/10.1073/pnas.1604824113.

Sears, Michael W, Evan Raskin, and Michael J Angilletta. 2011. "The World Is Not Flat: Defining Relevant Thermal Landscapes in the Context of Climate Change." *Integrative and Comparative Biology* 51 (5): 666–75. https://doi.org/10.1093/icb/icr111.

Shah, Alisha A., Michael E. Dillon, Scott Hotaling, and H. Arthur Woods. 2020. "High Elevation Insect Communities Face Shifting Ecological and Evolutionary Landscapes." *Current Opinion in Insect Science* 41: 1–6. https://doi.org/10.1016/j.cois.2020.04.002.

Shinneman, Douglas J., William L. Baker, Paul C. Rogers, and Dominik Kulakowski. 2013. "Fire Regimes of Quaking Aspen in the Mountain West." *Forest Ecology and Management* 299: 22–34. https://doi.org/10.1016/j.foreco.2012.11.032.

Singsaas, Eric L., Marianne M. Laporte, Jain Zhong Shi, Russell K. Monson, David R. Bowling, Kristine Johnson, Manuel Lerdau, Amal Jasentuliytana, and Thomas D. Sharkey. 1999. "Kinetics of Leaf Temperature Fluctuation Affect Isoprene Emission from Red Oak (Quercus Rubra) Leaves." *Tree Physiology* 19 (14): 917–24.

https://doi.org/10.1093/treephys/19.14.917.

Sommer, Stefan, and R??diger Wehner. 2012. "Leg Allometry in Ants: Extreme Long-Leggedness in Thermophilic Species." *Arthropod Structure and Development* 41 (1): 71–77.

Stahlschmidt, Zachary R., and Shelley A. Adamo. 2013. "Warm and Cozy: Temperature and Predation Risk Interactively Affect Oviposition Site Selection." *Animal Behaviour*. https://doi.org/10.1016/j.anbehav.2013.06.009.

Stoutjesdijk, P. 1977. "High Surface Temperatures of Trees and Pine Litter in the Winter and Their Biological Importance." *International Journal of Biometeorology*. https://doi.org/10.1007/BF01555192.

Sunday, Jennifer M, Amanda E Bates, Michael R Kearney, Robert K Colwell, Nicholas K Dulvy, John T Longino, and Raymond B Huey. 2014. "Thermal-Safety Margins and the Necessity of Thermoregulatory Behavior across Latitude and Elevation." *Proceedings of the National Academy of Sciences of the United States of America* 111 (15): 5610–15. https://doi.org/10.1073/pnas.1316145111.

Vance, L.K., and T. Luna. 2017. "Rocky Mountain Dry-Mesic Montane Mixed Conifer Forest — Northern Rocky Mountain Dry-Mesic Montane Mixed Conifer Forest. Montana Field Guide." Montana Natural Heritage Program. 2017. http://fieldguide.mt.gov/displayES_Detail.aspx?ES=4232.

Vogel, Steven. 2009. "Leaves in the Lowest and Highest Winds: Temperature, Force and Shape." *New Phytologist* 183 (1): 13–26. https://doi.org/10.1111/j.1469-8137.2009.02854.x.

Wagner, Diane, Linda DeFoliart, Patricia Doak, and Jenny Schneiderheinze. 2008. "Impact of Epidermal Leaf Mining by the Aspen Leaf Miner (Phyllocnistis Populiella) on the Growth, Physiology, and Leaf Longevity of Quaking Aspen." *Oecologia* 157 (2): 259–67. https://doi.org/10.1007/s00442-008-1067-1.

Wagner, Diane, Jenifer M. Wheeler, and Stephen J. Burr. 2020. "The Leaf Miner Phyllocnistis Populiella Negatively Impacts Water Relations in Aspen." *Tree Physiology* 40 (5): 580–90. https://doi.org/10.1093/TREEPHYS/TPZ109.

Welter, Stephen C. 2019. "Arthropod Impact on Plant Gas Exchange." In *Insect-Plant Interactions*, 135–64. https://doi.org/10.1201/9780429290916-5.

Williams, Caroline M., Hugh A.L. Henry, and Brent J. Sinclair. 2015. "Cold Truths: How Winter Drives Responses of Terrestrial Organisms to Climate Change." *Biological Reviews* 90 (1): 214–35. https://doi.org/10.1111/brv.12105.

Willmer, P.G. 1982. "Microclimate and the Environmental Physiology of Insects." *Advances in Insect Physiology* 16: 1–57.

Woods, H. Arthur. 2013. "Ontogenetic Changes in the Body Temperature of an Insect Herbivore." *Functional Ecology* 27 (6): 1322–31. https://doi.org/10.1111/1365-2435.12124.

Woods, H. Arthur, Michael E. Dillon, and Sylvain Pincebourde. 2015. "The Roles of Microclimatic Diversity and of Behavior in Mediating the Responses of Ectotherms to Climate Change." *Journal of Thermal Biology* 54: 86–97. https://doi.org/10.1016/j.jtherbio.2014.10.002.

Woods, H. Arthur, Geoffrey Legault, Joel Kingsolver, Sylvain Pincebourde, Alisha Shah, &

Beau Larkin. 2022a. Climate-driven thermal opportunities and risks for leaf miners in aspen canopies. Dryad, dataset. https://doi.org/10.5061/dryad.d2547d84j

Woods, H. Arthur, Geoffrey Legault, Joel Kingsolver, Sylvain Pincebourde, Alisha Shah, & Beau Larkin. 2022b. Climate-driven thermal opportunities and risks for leaf miners in aspen canopies. Zenodo, software. https://doi.org/10.5281/zenodo.6613812

Woods, H. Arthur, Sylvain Pincebourde, Michael E. Dillon, and John S. Terblanche. 2021. "Extended Phenotypes: Buffers or Amplifiers of Climate Change?" *Trends in Ecology & Evolution*. https://doi.org/10.1016/j.tree.2021.05.010.

Woods, H. Arthur, Marc Saudreau, and Sylvain Pincebourde. 2018. "Structure Is More Important than Physiology for Estimating Intracanopy Distributions of Leaf Temperatures." *Ecology and Evolution* 8 (10): 5206–18. https://doi.org/10.1002/ece3.4046.

Yang, Jian, Peter J. Weisberg, Douglas J. Shinneman, Thomas E. Dilts, Susan L. Earnst, and Robert M. Scheller. 2015. "Fire Modulates Climate Change Response of Simulated Aspen Distribution across Topoclimatic Gradients in a Semi-Arid Montane Landscape." *Landscape Ecology* 30 (6): 1055–73. https://doi.org/10.1007/s10980-015-0160-1.

Young, D. R., and W. K. Smith. 1979. "Influence of Sunflecks on the Temperature and Water Relations of Two Subalpine Understory Congeners." *Oecologia* 43 (2): 195–205. https://doi.org/10.1007/BF00344770.

Zangerl, A. R., J. G. Hamilton, T. J. Miller, A. R. Crofts, K. Oxborough, M. R. Berenbaum, and E. H. De Lucia. 2002. "Impact of Folivory on Photosynthesis Is Greater than the Sum of Its Holes." *Proceedings of the National Academy of Sciences of the United States of America* 99 (2): 1088–91. https://doi.org/10.1073/pnas.022647099.

Zellweger, Florian, Pieter de Frenne, Jonathan Lenoir, Pieter Vangansbeke, Kris Verheyen, Markus Bernhardt-Römermann, Lander Baeten, et al. 2020. “Forest Microclimate Dynamics Drive Plant Responses to Warming.” *Science* 368 (6492): 772–75. https://doi.org/10.1126/science.aba6880.

Tables

Table 1. ANOVA summary of linear mixed-effects model examining the main effects tissue type (mined or unmined), light condition (shade, partial shade, or full sun), and their interaction for 68 leaves.

	numDF	denDF	F	P
Intercept	1	65	0.3	0.59
Tissue (mined vs unmined)	1	65	174.6	<0.0001
Light condition	2	65	63.7	<0.0001
Tissue × light condition	2	65	4.1	0.022

Table 2. ANOVA summary of linear mixed-effects model examining the effects on $\log_{10}$ growth rate of initial larval mass, treatment (whether leaves were experimentally shaded or not), time of day, and the interaction between treatment and time of day. Initial mass did not interact significantly with other predictors and therefore interactions were not included.

	numDF	denDF	F	P
Intercept	1	142	1346.5	<0.0001
$\log_{10}$ Initial mass	1	142	386.8	<0.0001
Treatment (shaded or not)	1	27	0.2	0.65
Day or night	1	142	22.4	<0.0001
Treatment × Day or night	1	142	1.8	0.18

Figure Legends.

Figure 1. (A) Thermal performance curve, showing performance rising from zero (at CT_{MIN}, near 0 °C) to a maximum value at T_{OPT}. Performance falls rapidly at temperatures above T_{OPT}, reaching zero at CT_{MAX}. (B) Distributions of locally available body temperatures (shown as density plots) available spatially among microsites. In cold conditions (blue), e.g. in early in spring or during cold weather, insects may be so cold that performance is strongly depressed or approaches zero (CT_{MIN}). Likewise, in warm conditions (red), e.g. in mid-summer or during particularly hot weather, insects may be so hot that performance declines to zero. Mobile insects may be able to move short distances and achieve much more favorable body temperatures, especially if sunny and shady locations are available. Immobile insects (pupae, or larvae that are restricted to mines, galls, or other structures) may be able to anticipate and minimize the effects of extreme microclimatic conditions by building structures or engineering the tissues of their host plants.

Figure 2. Mine and larva on aspen leaf. The larva has completed feeding and growth and is about to construct a pupation chamber on the leaf margin (A). Box containing battery and computer that controls the heating box used to heat shock larvae (B). Close up of mined leaf and larva inside a heating box (C). A pair of leaf mines, one shaded by a rectangle of plastic and foil (D).

Figure 3. Temperature distributions of leaves that were experimentally shaded or not. (A) Example trace of a pair of leaves during the first experimental period (May 22 – 25, 2018). Over much of the diurnal cycle, temperatures of sun-exposed (orange) and shaded (gray) leaves were similar and were driven by diurnal changes in air temperature. During the daytime, however, the temperature of the sun-exposed leaf sometimes spiked higher. (B and C) Distributions of leaf

temperatures (shown as density plots, smoothing bandwidth = 1) for each of 10 sun-exposed (orange lines) and 10 shaded leaves (gray lines), with means shown in black for shaded and dark orange for exposed leaves. The bimodal shape reflects that nighttime temperatures are centered at 10 °C and daytime temperatures at 20 °C. The daytime spikes to higher temperatures in sun-exposed leaves are indicated by right-shifted orange lines above 25 °C.

Figure 4. (A) Leaf temperature and (B) difference in temperature between paired sun-exposed and shaded leaves as functions of air temperature measured at a nearby weather station.

Figure 5. Temperatures of mined and unmined tissues on single leaves (N = 68) in three different lighting conditions, shade, partial shade, and full sun.

Figure 6. Log_{10} larval mass as a function of log10 mine area. For analyses, data were pooled from 2017 (filled symbols) and 2018 (empty symbols). In 2017, we analyzed primarily larger mines and larvae; in 2018, we extended the size ranges to include small mines and larvae.

Figure 7. (A) Box plots of mass-specific growth rates of shaded (black) or sun-exposed (orange) larvae during five successive day-night periods (N = 55 larvae), excluding those that grew less than 5 µg/mg/hour over the course of the experiment. (B) Growth rates of each larva in each time period (daytime in red, nighttime in blue) plotted as a function of its mass at the beginning of the period. Gray lines connect subsequent measurements within each larva. Those for which there are fewer than five points died or disappeared during the experiment.

Figure 8. Response (alive or dead) of leaf-miner larvae subjected to a 1-h heat shock in situ in their leaf still connected to the tree. Mortality was assessed 48 h later. To improve visibility, data points are jittered vertically. A fitted logistic regression estimated that the LT_{50} (temperature killing 50% of larvae) was 42.1 °C, and the highest temperature survived was 43.1 °C.

Figure 9. Growth rates of larval *P. populiella* during 8 hours of exposure to constant temperatures in incubators. Mined leaves were picked from trees at our field site the day before and returned to the lab and held overnight at a common temperature (10 °C) before measurements. Violin plots show the prediction densities for maximum rates (non-molting, red) and for realized switching rates (with transitions between molting states, green), derived from the fitted two-state model. See Appendix S1 for details.

Figure 10. The size (A) and temperature (B) dependence of bite rate by aspen leaf miners. Larvae were observed under a stereomicroscope and bites per minute determined. (A) Considering bite rates (N = 41 larvae) obtained just between 22 and 28 °C, larger larvae ate significantly faster than did small larvae. (B) Larval bite rates were highest near 25 °C, with a broad optimum, and bite rates fell to zero between 35 and 40 °C. Gray dots and lines are for individual larvae, and the black line is the fitted thermal performance curve (N = 39 larvae). The dot and error bars near 40 °C estimate the mean and 95% CI of CT_{MAX} (39.9 °C, 38.5 – 41.3 °C).

Figure 11. Proportion of sun-exposed or experimentally shaded mines exceeding high-temperature thresholds between 1999 and 2020. Filled dots show the proportion of mines in which temperatures exceed thresholds when the actual daily maximum air temperatures were used. Open dots show the proportion of mines under a warming regime, in which 3 °C was added to the recorded daily maximum temperatures. Shaded polygons track the maximum proportion among all years under the actual temperature scenario (dark gray) and the warmed temperature regime (light gray). To improve clarity, proportions of zero were excluded. 4048 values are possible for each panel (92 days each year, 22 years, 2 temperature regimes). From top-left to bottom right, the number of values that exceed zero are 923 (23%), 2086 (52%), 493 (12%), and 1578 (39%).

Figure 12. Distributions of simulated daily leaf consumption (highly correlated with growth, see Figure 6) by leaf-mining larvae based on mean hourly measured air temperatures from the weather station at MPG-North for the years 2017 – 2019 (mid-May to mid-June only). Simulations used the fitted two-state feeding/growth model shown in Figure 9 and described in Appendix S1: Section S1.

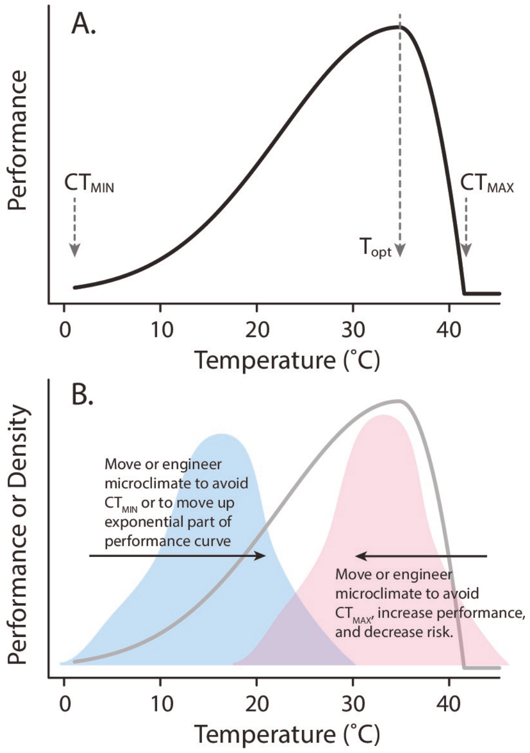

Move or engineer microclimate to avoid CT_{MIN} or to move up exponential part of performance curve

Move or engineer microclimate to avoid CT_{MAX}, increase performance, and decrease risk.

figure 1.ai


A.
B.
C.
D.

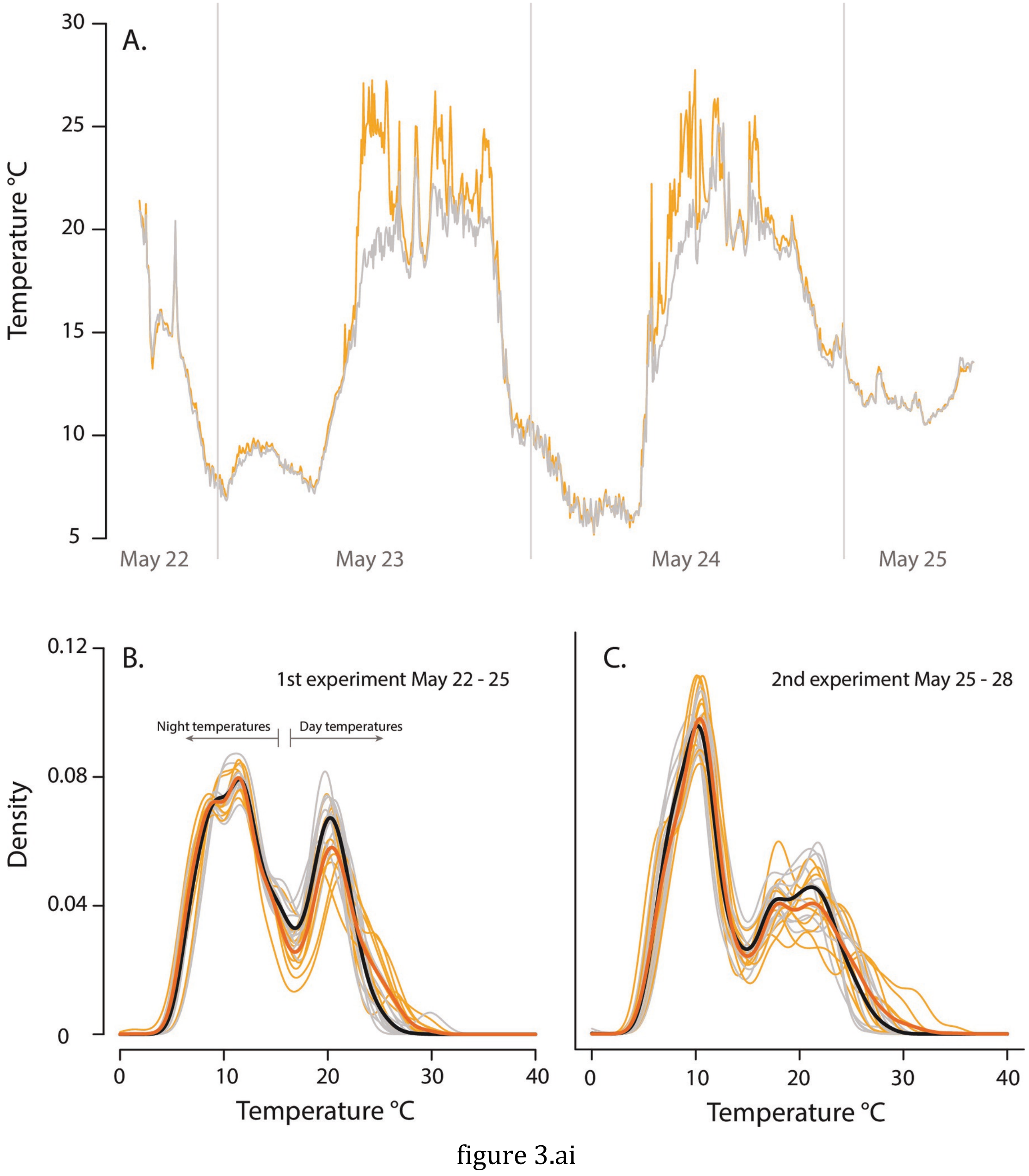
A.
Temperature °C
30
25
20
15
10
5
May 22
May 23
May 24
May 25
B.
1st experiment May 22 - 25
Night temperatures
Day temperatures
Density
0.12
0.08
0.04
0
0
10
20
30
40
Temperature °C
C.
2nd experiment May 25 - 28
0
10
20
30
40
Temperature °C

figure 3.ai

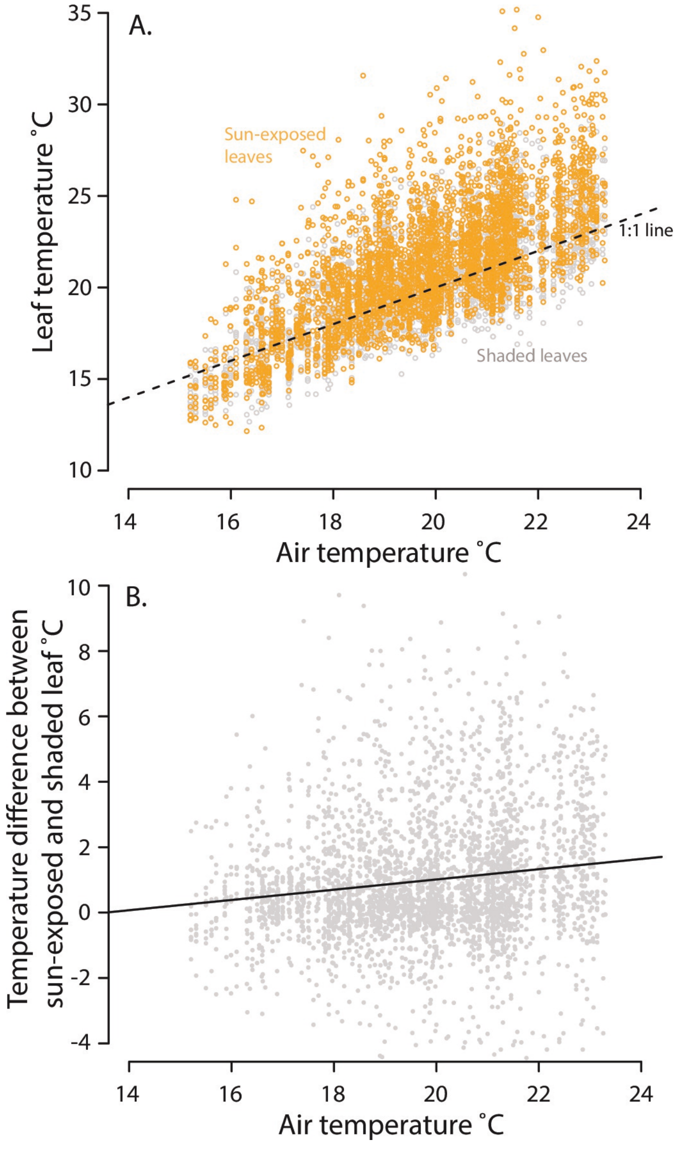
A.
Leaf temperature ˚C
35
30
25
20
15
10
Sun-exposed leaves
1:1 line
Shaded leaves
14
16
18
20
22
24
Air temperature ˚C
B.
Temperature difference between sun-exposed and shaded leaf ˚C
10
8
6
4
2
0
-2
-4
14
16
18
20
22
24
Air temperature ˚C

figure 4.ai

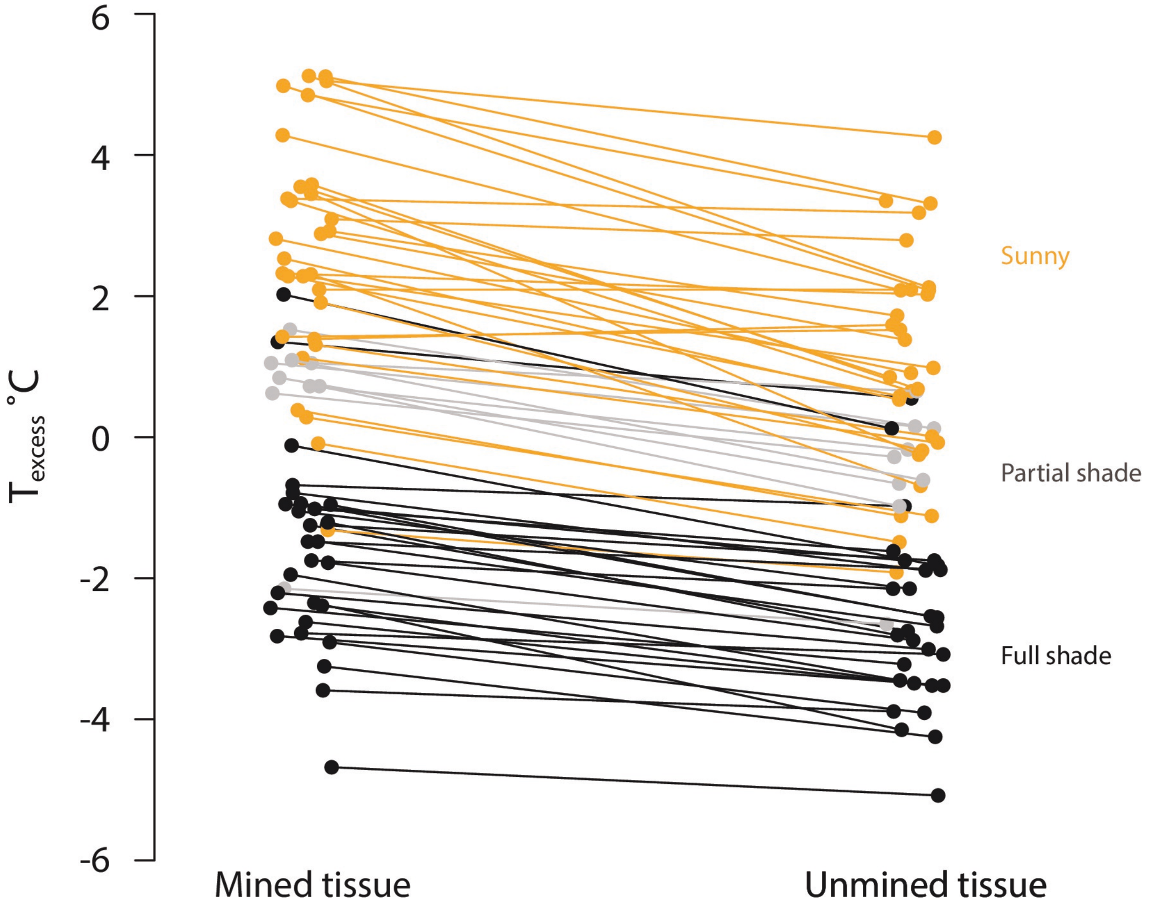
6
4
2
0
-2
-4
-6
T_{excess} °C
Sunny
Partial shade
Full shade
Mined tissue
Unmined tissue

figure 5.ai

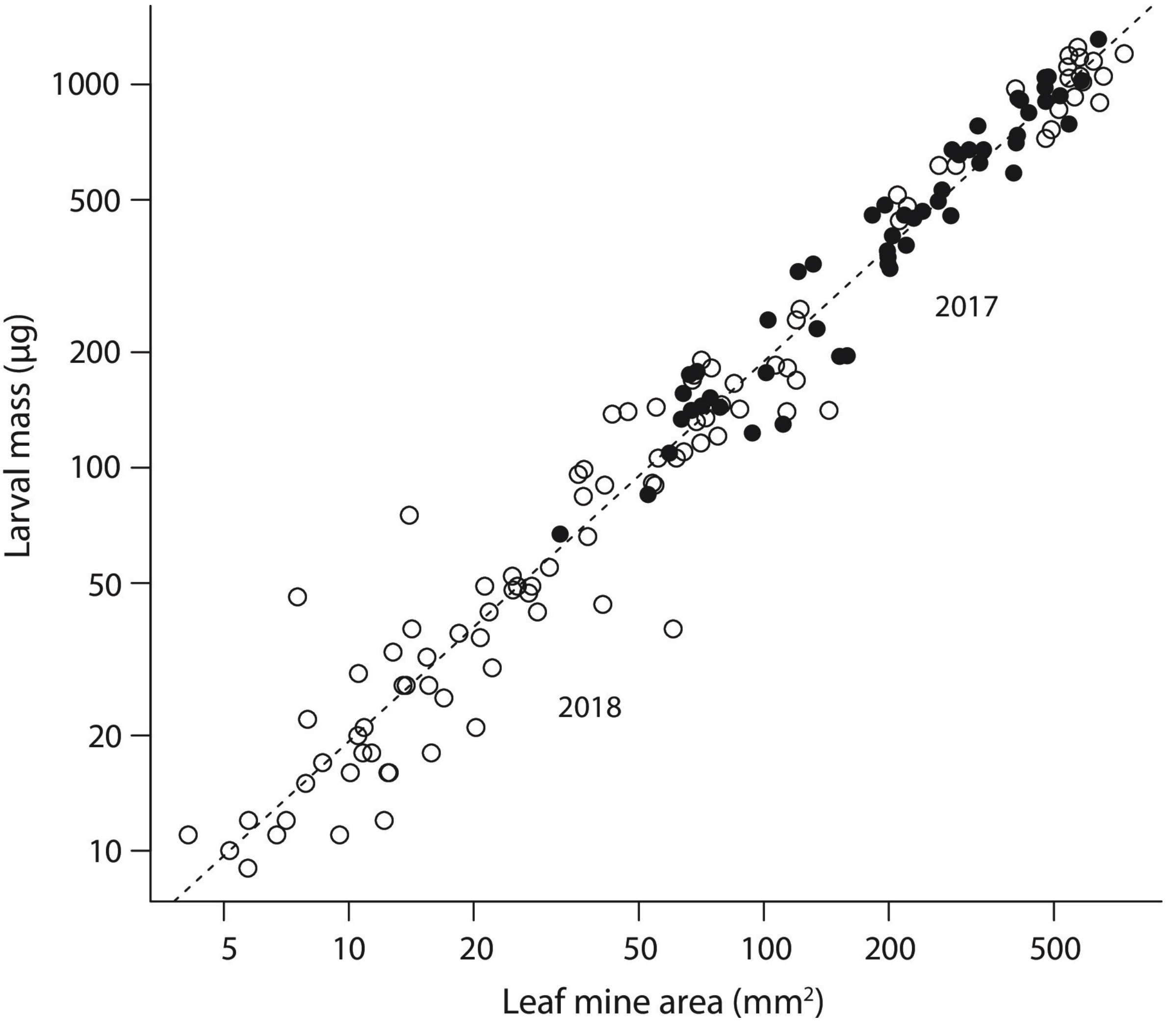
Larval mass (µg)
1000
500
200
100
50
20
10
2017
2018
5
10
20
50
100
200
500
Leaf mine area (mm²)

figure 6.ai

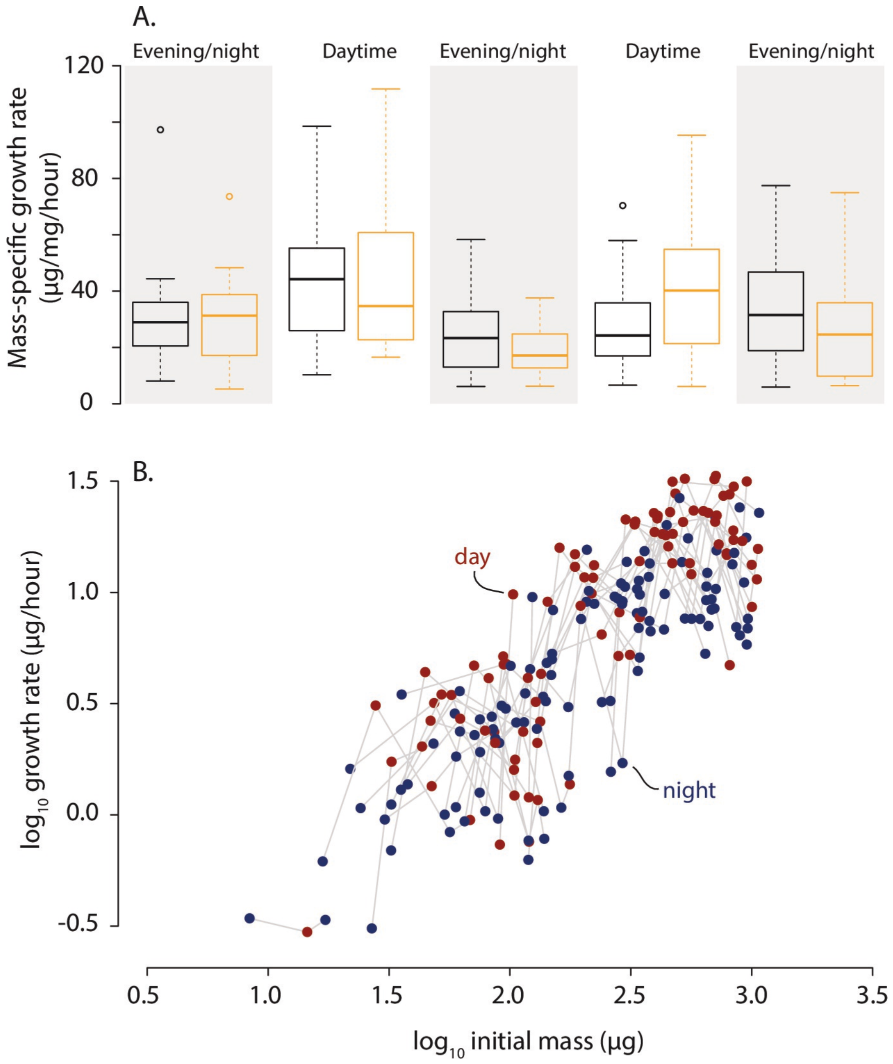
A.
Evening/night
Daytime
Evening/night
Daytime
Evening/night
Mass-specific growth rate (μg/mg/hour)
0
40
80
120
B.
day
night
log10 growth rate (μg/hour)
-0.5
0.0
0.5
1.0
1.5
log10 initial mass (μg)
0.5
1.0
1.5
2.0
2.5
3.0
3.5

figure 7.ai

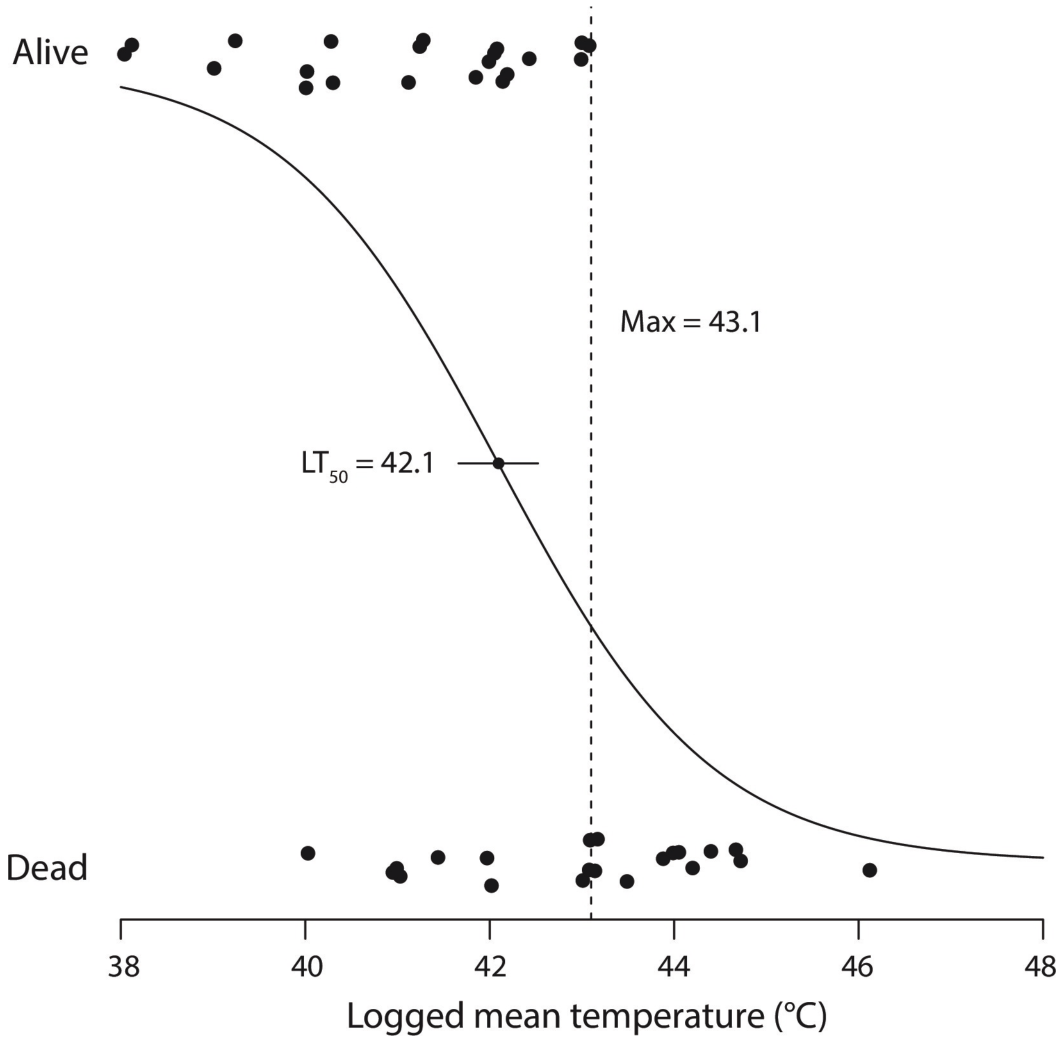
Alive
Dead
Max = 43.1
LT_{50} = 42.1
38
40
42
44
46
48
Logged mean temperature (°C)

figure 8.ai

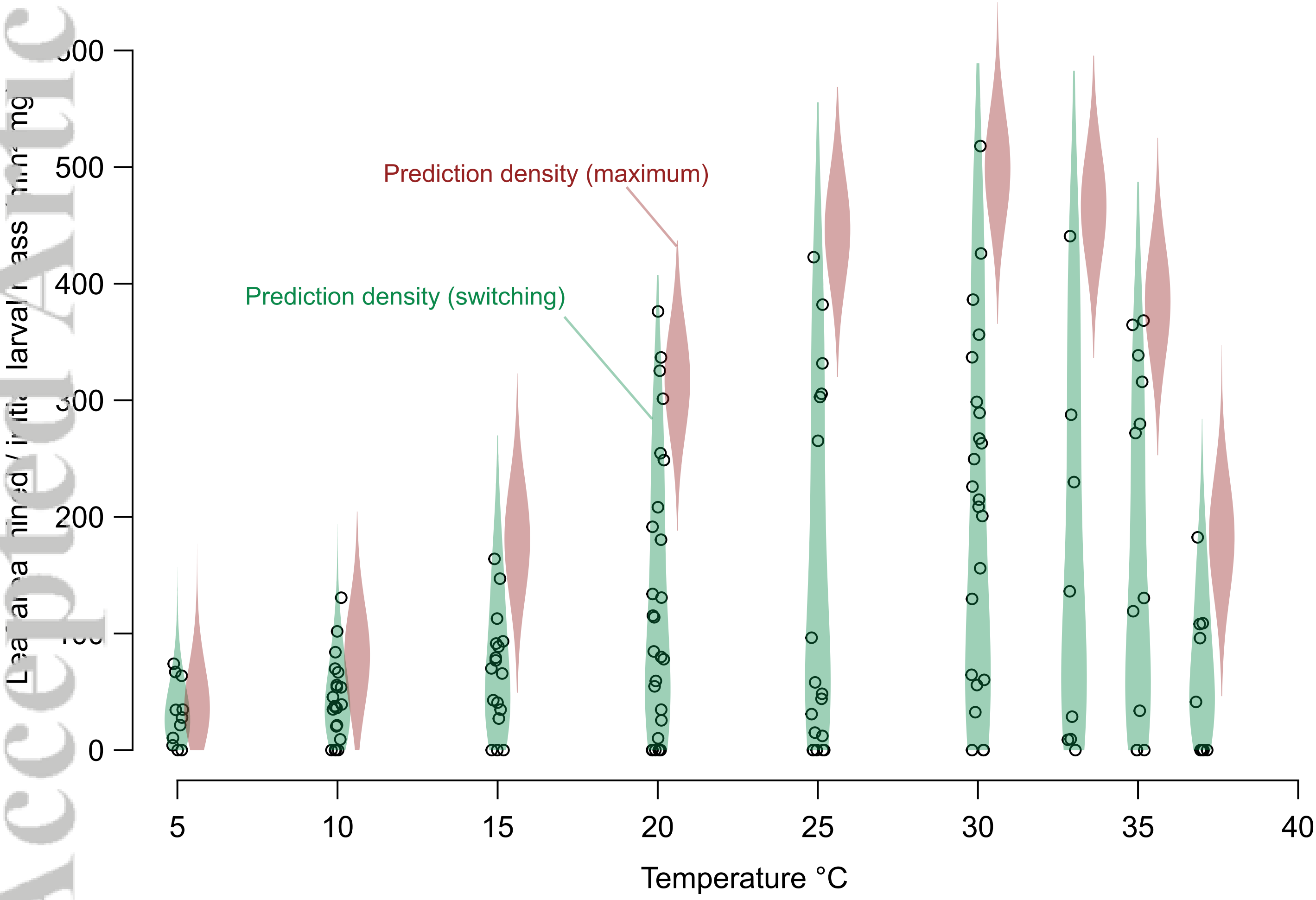
Prediction density (maximum)
Prediction density (switching)
0
100
200
300
400
500
600
5
10
15
20
25
30
35
40
Temperature °C

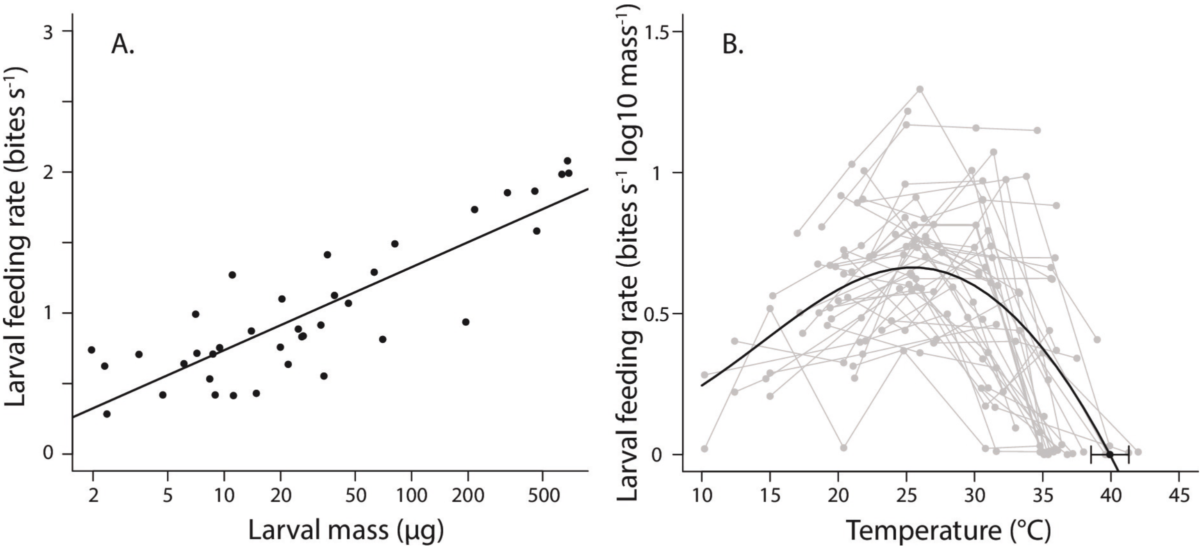
A.
Larval feeding rate (bites s^{-1})
0
1
2
3
Larval mass (µg)
2
5
10
20
50
100
200
500
B.
Larval feeding rate (bites s^{-1} log10 mass^{-1})
0
0.5
1
1.5
Temperature (°C)
10
15
20
25
30
35
40
45

figure 10.ai

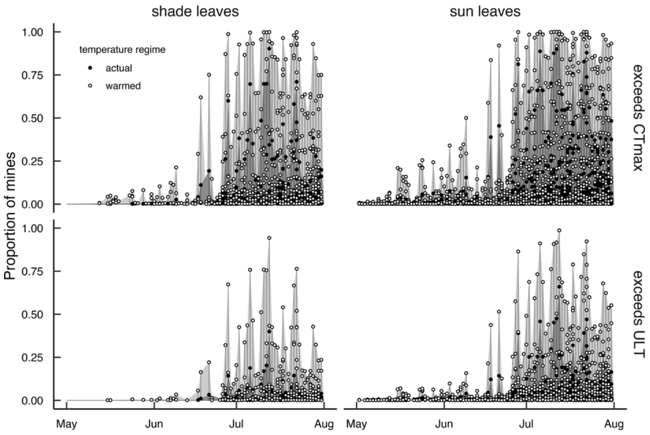

Figure_11.tiff

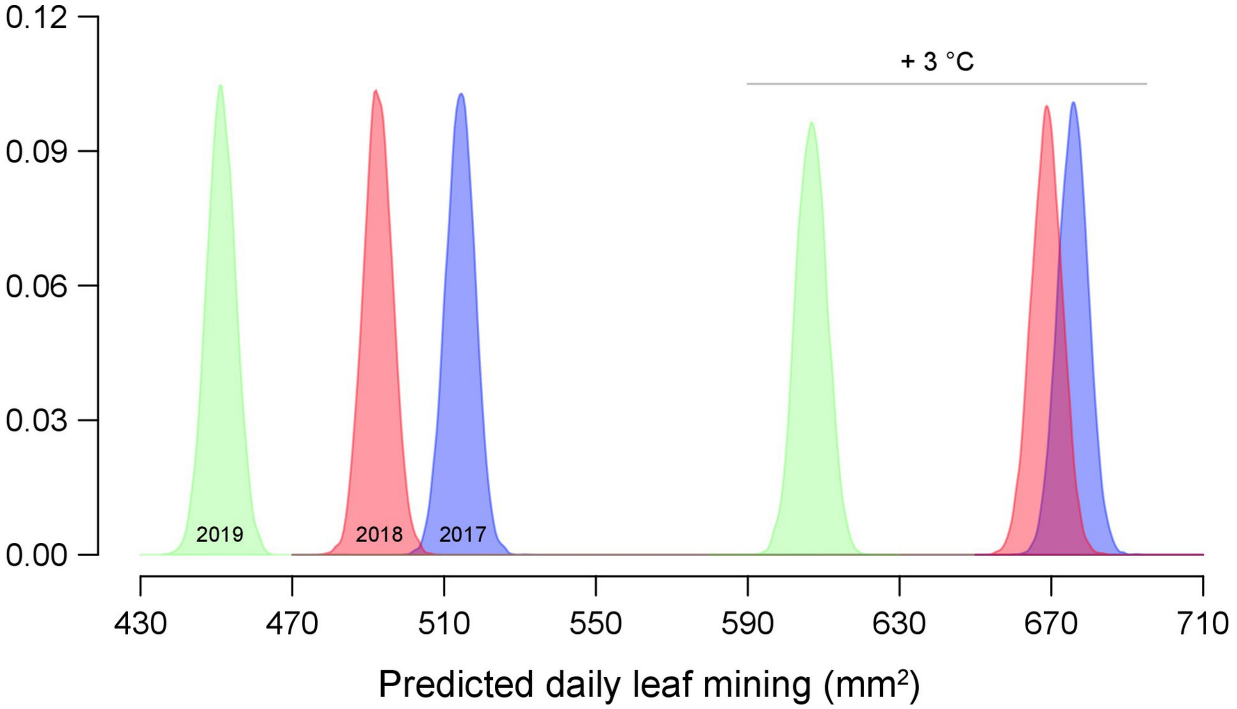
0.12
0.09
0.06
0.03
0.00
Density
+ 3 °C
2019
2018
2017
430
470
510
550
590
630
670
710
Predicted daily leaf mining (mm²)

figure 12.ai